Dysbiosis-induced intestinal inflammation activates TNFRI and mediates alcoholic liver disease in mice

Peng Chen[1], Peter Stärkel[2], Jerrold R. Turner[3], Samuel B. Ho [1,4], and Bernd Schnabl[1]

[1]Department of Medicine, University of California San Diego, La Jolla, CA,

[2]St. Luc University Hospital, Université Catholique de Louvain, Brussels, Belgium,

[3]Department of Pathology, The University of Chicago, Chicago, IL,

[4]Department of Medicine, VA San Diego Healthcare System, San Diego, CA

Correspondence: Bernd Schnabl, M.D., Department of Medicine, University of California San Diego, MC0063, 9500 Gilman Drive, La Jolla, CA 92093, Phone 858-822-5311, Fax 858-822-5370, Email beschnabl@ucsd.edu

Short title: Intestinal injury in alcoholic liver disease

Keywords: TNFα, endotoxin, intestinal injury, microbiome, microbiota, steatohepatitis

Abbreviations: ADH, alcohol dehydrogenase; ALT, alanine aminotransferase; CYP2E1, cytochrome p450 enzyme 2E1; *E.coli, Escherichia coli;* FACS, fluorescence-activated cell sorting; MLCK, myosin light chain kinase, TNFα, tumor necrosis factor alpha; TNFRI, tumor necrosis factor receptor I; VDAC1, Voltage-dependent anion-selective channel protein 1.

None of the authors has a financial, personal or professional conflict of interest to disclose.

Abstract

Intestinal barrier dysfunction is an important contributor to alcoholic liver disease. Translocated microbial products trigger an inflammatory response in the liver and contribute to steatohepatitis. Our aim was to investigate mechanisms of barrier disruption following chronic alcohol feeding. A Lieber-DeCarli model was used to induce intestinal dysbiosis, increased intestinal permeability and liver disease in mice. Alcohol feeding for 8 weeks induced intestinal inflammation in the jejunum, which is characterized by an increased number of TNFα producing monocytes and macrophages. These findings were confirmed in duodenal biopsies from patients with chronic alcohol abuse. Intestinal decontamination with non-absorbable antibiotics restored eubiosis, decreased intestinal inflammation and permeability, and reduced alcoholic liver disease in mice. TNF-receptor I (TNFRI) mutant mice were protected from intestinal barrier dysfunction and alcoholic liver disease. To investigate whether TNFRI on intestinal epithelial cells mediates intestinal barrier dysfunction and alcoholic liver disease, we used TNFRI mutant mice carrying a conditional gain-of-function allele for this receptor. Reactivation of TNFRI on intestinal epithelial cells resulted in increased intestinal permeability and liver disease that is similar to wild type mice after alcohol feeding, suggesting that enteric TNFRI promotes intestinal barrier dysfunction. Myosin light chain kinase (MLCK) is a downstream target of TNFα and was phosphorylated in intestinal epithelial cells following alcohol administration. Using MLCK deficient mice, we further demonstrate a partial contribution of MLCK to intestinal barrier dysfunction and liver disease following chronic alcohol feeding. In conclusion, dysbiosis-induced intestinal inflammation and TNFRI signaling on intestinal epithelial cells are mediating a disruption of the intestinal barrier. Therefore, intestinal TNFRI is a crucial mediator of alcoholic liver disease.

Introduction

Alcohol abuse is one of the leading causes of chronic liver disease and liver-related deaths worldwide. A prominent feature of alcohol abuse is disruption of the intestinal barrier function[1]. Increased intestinal permeability is present in preclinical animal models and in patients with alcohol abuse[2, 3]. Microbial products such as lipopolysaccharide (LPS) translocate from the intestinal lumen to the extra-intestinal space, blood and liver[4]. In the liver, bacterial products induce inflammation and synergize with ethanol-induced hepatotoxicity to cause steatosis, steatohepatitis and fibrosis[5]. Mice that express non-functional Toll-like receptor 4 (TLR4) or non-functional molecules of the LPS signaling pathway are protected from experimental alcoholic liver disease[6]. Levels of LPS in the portal vein of mice with a non-functional TLR4 expression are similar to wild type mice, indicating that TLR4 does not control intestinal permeability and that protection from disease occurs at the level of the liver.

The exact molecular mechanism of increased intestinal permeability during alcoholic liver disease is not known. Acetaldehyde as major oxidative metabolite of ethanol induces Caco-2 cell monolayer disruption by tight junction protein redistribution[7], and several potential mediators such as Snail, protein phosphatase 2A (PP2A), extracellular-signal-regulated kinase (ERK), protein kinase C (PKC), and protein tyrosine phosphatase (PTPase) are involved[8-12]. In addition, increased inducible nitric oxide synthases (iNOS) and myosin light chain kinase (MLCK) expression correlated with barrier function disruption in differentiated Caco-2 cells[13, 14]. Most studies are using cell culture systems, and there are no *in vivo* data investigating the pathway that induces intestinal barrier disruption following chronic alcohol administration.

In the current study, we use an animal model of chronic alcoholic liver disease to demonstrate that intestinal dysbiosis induces tumor necrosis factor α (TNFα) production in inflammatory cells of the intestinal lamina propria. TNF-receptor

I (TNFRI) on intestinal epithelial cells mediates tight junction disruption partially by activation of MLCK.

Materials and Methods

Animal models of alcohol feeding. TNFRI$^{flxneo/flxneo}$, VillinCreTNFRI$^{flxneo/flxneo}$ and MLCK deficient mice have been described and were all on a C57BL/6 genetic background. TNFRI$^{flxneo/flxneo}$ [15] and VillinCreTNFRI$^{flxneo/flxneo}$ [16] were kindly provided by Drs. Manolis Roulis and George Kollias (Biomedical Sciences Research Center 'Alexander Fleming', Vari, Greece), and littermates were used for the experiments. C57BL/6 wild type mice were bred in the same room of our vivarium and used as controls for experiments involving TNFRI$^{flxneo/flxneo}$ and VillinCreTNFRI$^{flxneo/flxneo}$ mice. TNFR2 deficient mice were originally obtained from Jackson lab, and were kindly provided by Dr. William McBride (University of California Los Angeles). Heterozygous long MLCK$^{-/-}$ mice[17] were crossed, and wild type and knockout littermates were used for all experiments. The Lieber DeCarli diet model of alcohol feeding was used for 8 weeks.

Other materials and methods are described in the Supplementary Materials and Methods section.

Results

Chronic alcohol feeding enhances TNFα expression in the jejunum of mice. TNFα disrupts intestinal tight junctions and is a well characterized mediator of intestinal barrier dysfunction[18]. We therefore assessed whether intestinal TNFα is increased in an animal model of chronic alcohol feeding for 8 weeks. TNFα gene expression was significantly induced in the jejunum of alcohol-fed mice compared with isocaloric controls (Fig. 1A). Because intestinal inflammation caused by inflammatory cells in the lamina propria is involved in increasing intestinal

permeability[19], lamina propria cells were isolated and separated from epithelial cells. Increased jejunal TNFα was due to an induction of gene expression in isolated lamina propria cells of mice subjected to alcohol feeding (Fig. 1B). FACS analysis was used to further characterize the innate immune cell infiltrate producing TNFα. The number of $TNF\alpha^+$ monocytes and macrophages, but not dendritic cells, was significantly increased in the jejunum after 8 weeks of alcohol feeding (Fig. 1C). $TNF\alpha^+$ innate immune cells were not elevated in the ileum and colon following ethanol administration in mice (Suppl. Fig. 1). Moreover, the absolute number of monocytes, macrophages or dendritic cells was not significantly elevated in the small or large intestine after alcohol administration (Suppl. Fig. 2). These results indicate that the induction of TNFα expression does not result from an increased infiltration of innate immune cells, but is rather a consequence of innate immune cell activation.

Alcohol abuse increases TNFα production of intestinal monocytes and macrophages in humans. To confirm these results in humans, duodenal biopsies from healthy individuals and patients with chronic alcohol abuse were examined. Similar to findings in our preclinical model of alcoholic liver disease, TNFα mRNA expression was significantly higher in duodenal biopsies from alcoholics (Fig. 2A). Using CD68 that is primarily expressed by human monocytes and macrophages, immunofluorescent staining demonstrated a significant increase of CD68/TNFα double positive cells in the lamina propria of alcoholic patients (Fig. 2B and C). Due to limited availability of jejunal, ileal and colonic samples from alcoholics, our experiments are restricted to the examination of duodenal samples. These data suggest that chronic alcohol consumption results in increased intestinal TNFα production in humans.

Enteric dysbiosis induces intestinal TNFα during alcoholic liver disease development. We and others have recently shown that chronic alcohol feeding results in dysbiosis with qualitative and quantitative disturbances in the microbiome using an intragastric feeding model for 3 weeks or Lieber-DeCarli feeding,

respectively[20-22]. Interestingly, intestinal permeability is significantly increased in the jejunum after alcohol feeding (Suppl. Fig. 3), and intestinal bacterial overgrowth is most pronounced in the jejunum[20], the intestinal site with elevated levels of TNFα. Since dysbiosis is associated with intestinal inflammation[23], we next investigated whether restoration of eubiosis abolishes the induction of intestinal TNFα. Mice were subjected to alcohol or isocaloric diet feeding, and depletion of the commensal microflora was performed using non-absorbable antibiotics Polymyxin B and Neomycin for the last 4 weeks. Intestinal bacterial overgrowth was induced following alcohol feeding, but completely abolished in mice receiving non-absorbable antibiotics and subjected to alcohol feeding (Fig. 3A). Importantly, reducing the intestinal bacterial burden significantly reduced intestinal TNFα expression after chronic alcohol feeding (Fig. 3B). Consistent with gene expression data, non-absorbable antibiotics reduced the number of TNFα positive monocytes and macrophages in the lamina propria of the jejunum (Fig. 3C,D). Moreover, the intestinal barrier was stabilized by preventing a decrease of the tight junction protein occludin following chronic alcohol administration (Fig. 3E). Non-absorbable antibiotics prevented an increase of intestinal permeability in alcohol-fed mice as determined by fecal albumin ELISA (Fig. 3F). We confirmed previously published results from rats that intestinal decontamination reduces alcoholic liver disease[24] as evidenced by decreased liver injury (Suppl. Fig. 4A) and steatosis (Suppl. Fig. 4B, C). Additionally, oral antibiotics restore liver/body weight ratio (Suppl. Fig. 5A), but did not alter intestinal ethanol absorption (Suppl. Fig. 5B). Using a time course experiment, we found that intestinal inflammation precedes the onset of increased intestinal permeability (Fig. 3G, H). We assessed whether changes in the epithelial integrity contributes to gut barrier dysfunction, but found that the morphology of intestinal villi was normal in the jejunum after chronic alcohol feeding (Suppl. Fig. 6A). In addition, there was no significant difference in the apoptosis rate of jejunal enterocytes between control and alcohol mice (Suppl. Fig. 6B). Our findings suggest that alcohol-associated enteric dysbiosis induces intestinal inflammation and increases intestinal permeability.

TNFRI on enterocytes induces intestinal barrier dysfunction following chronic alcohol feeding. To further define the role of TNFα in mediating intestinal barrier dysfunction following alcohol administration, we focused on the main receptor for TNFα, TNF-receptor I (TNFRI). Since experimental alcoholic liver disease depends on increased intestinal permeability and translocation of microbial products from the intestinal lumen to the liver[4], we investigated the contribution of TNFRI expressed on enterocytes to intestinal barrier regulation. We used mutant mice carrying a conditional gain-of-function allele for TNFRI with an introduced loxP-flanked neomycin-resistance cassette in intron 5 of the murine *p55TnfR* gene ($TNFRI^{flxneo/flxneo}$)[15]. A nonfunctional TNFRI allele is engineered to be reactivated specifically in villin expressing intestinal epithelial cells by a Villin Cre-loxP-mediated recombination. By crossing $TNFRI^{flxneo/flxneo}$ mice with the intestinal epithelial cell specific VillinCre transgenic mouse, a functional TNFRI is selectively expressed on intestinal epithelial cells ($VillinCreTNFRI^{flxneo/flxneo}$)[16, 25], while all other tissues and organs (including the liver) are mutant for TNFRI. We confirmed by western blotting that TNFRI is absent in intestinal epithelial cells isolated from TNFRI mutant $TNFRI^{flxneo/flxneo}$ mice, while TNFRI was reactivated and expressed on enterocytes isolated from $VillinCreTNFRI^{flxneo/flxneo}$ mice (Suppl. Fig. 7A). In addition, TNFRI was not expressed in the liver of both strains. Wild type mice showed TNFRI expression on intestinal epithelial cells and in the liver (Suppl. Fig. 7A and B).

TNFRI mutant ($TNFRI^{flxneo/flxneo}$) mice were protected from an increase in intestinal permeability following alcohol feeding for 8 weeks compared with wild type mice as measured by fecal albumin. Levels of fecal albumin were significantly higher in mice with a selective reactivation of TNFRI on intestinal epithelial cells ($VillinCreTNFRI^{flxneo/flxneo}$) as compared with TNFRI mutant ($TNFRI^{flxneo/flxneo}$), but similar to C57BL/6 wild type mice (Fig. 4A). Hepatic contents of *E. Coli* proteins were determined as measure of bacterial translocation originating from the intestine. After alcohol feeding, livers from $TNFRI^{flxneo/flxneo}$ mice showed significantly less translocated *E. Coli* proteins as compared with wild type mice. However, $VillinCreTNFRI^{flxneo/flxneo}$ mice demonstrated more *E. Coli* translocation than their

TNFRI$^{flxneo/flxneo}$ littermates (Fig. 4B). Changes in tight junction protein expression are mediating the paracellular leakage pathway in the intestine. We therefore assessed protein level and integrity of the tight junction protein occludin in the jejunum using western blotting and immunofluorescence. Wild type mice showed a lower protein expression of occludin following ethanol feeding for 8 weeks as compared with isocaloric diet fed mice. While TNFRI$^{flxneo/flxneo}$ mice carrying a mutation in TNFRI are protected from tight junction disruption in the jejunum, VillinCreTNFRI$^{flxneo/flxneo}$ mice that have a functional TNFRI selectively expressed on intestinal epithelial cells, show a disruption of tight junction proteins (Fig. 4C-E). TNFRI expression in intestinal epithelial cells was not affected by alcohol feeding (Suppl. Fig. 8). TNFα mRNA level and TNFα protein expression by monocytes and macrophages were comparable in the jejunum of all groups after ethanol feeding (Suppl. Fig. 9). In contrast to a local secretion of TNFα by activated monocytes and macrophages in the intestinal lamina propria, it is also conceivable that systemic TNFα is elevated during alcoholic liver disease and activates TNFRI on intestinal epithelial cells to induce tight junction disruption. However, plasma TNFα levels were below the detection limit, both in control diet- and ethanol-fed mice (Suppl. Fig. 10). Taken together, mice with reactivation of TNFRI on enterocytes lose their protection against tight junction disruption as compared with TNFRI mutant mice suggesting that TNFRI on intestinal epithelial cells mediates intestinal barrier loss following chronic alcohol administration.

TNFRI on intestinal epithelial cells mediates alcoholic liver disease. We next determined whether changes in intestinal permeability directly translate into differences in alcoholic liver disease. Consistent with previous findings[26], TNFRI mutant (TNFRI$^{flxneo/flxneo}$) mice showed less liver injury as assessed by plasma ALT level (Fig. 5A, B) and decreased hepatic triglyceride contents after alcohol feeding compared with wild type mice (Fig. 5C, D), confirming that a non-functional TNFRI protects mice from alcoholic liver disease. VillinCreTNFRI$^{flxneo/flxneo}$ mice that have a functional TNFRI selectively on intestinal epithelial cells showed a significantly higher liver/body weight ratio (Suppl. Fig. 11A), more liver injury (Fig. 5A, B) and increased

hepatic steatosis (Fig. 5C, D) than TNFRI$^{flxneo/flxneo}$ mice, but comparable with wild type mice after chronic alcohol feeding. There is no significant difference in alcohol-induced liver injury and hepatic steatosis between VillinCreTNFRI$^{flxneo/flxneo}$ and wild type mice. Plasma ethanol levels (Fig. 5E) and hepatic ethanol metabolism (Suppl. Fig. 11B, C) were similar among the three groups of mice. In summary, TNFRI on intestinal epithelial cells contributes to the paracellular leakage pathway resulting in bacterial translocation, and promotes alcoholic liver disease.

Intestinal MLCK contributes to increased intestinal permeability and liver disease after chronic alcohol feeding. TNFα signaling phosphorylates and activates MLCK, which subsequently redistributes tight junction proteins and increases intestinal permeability in many intestinal diseases[14, 27]. To further identify TNFRI downstream signaling that mediates tight junction disruption following alcohol administration, we assessed phosphorylation of MLCK. Jejunal epithelial cells isolated from wild type mice that were administered alcohol by oral gavage once showed higher levels of phosphorylated MLCK (long isoform) than wild type mice gavaged with dextrose as control. This increase in MLCK phosphorylation was blunted in epithelial cells isolated from TNFRI mutant (TNFRI$^{flxneo/flxneo}$) mice following alcohol administration. Reactivation of TNFRI selectively on intestinal epithelial cells restored MLCK phosphorylation to a level similar to that of wild type mice after alcohol administration (Fig. 6A). However, MLCK phosphorylation is comparable between wild type and TNFR2 deficient enterocytes after ethanol administration (Suppl. Fig. 12). These data indicate that TNFRI, but not TNFR2 mediates MLCK activation in the intestinal epithelium after alcohol administration.

To dissect the functional role of MLCK in increasing intestinal permeability following chronic alcohol feeding, MLCK deficient and wild type littermate mice were subjected to the Lieber-DeCarli alcohol feeding model for 8 weeks. Alcohol feeding increased intestinal permeability in wild type mice as compared with isocaloric diet fed wild type mice. Intestinal permeability is significantly lower in MLCK$^{-/-}$ than wild type mice following alcohol administration. However, MLCK$^{-/-}$ mice still show higher levels

of fecal albumin compared with isocaloric diet fed mice (Fig. 6B). MLCK$^{-/-}$ mice showed a non-significant trend towards a lower amount of *E. Coli* proteins in the liver but significant lower LPS plasma level as compared with wild type littermates after alcohol feeding (Fig. 6C). Expression of occludin protein was diminished in the jejunum of alcohol-fed wild type mice, but not of alcohol-fed MLCK$^{-/-}$ mice (Fig. 6D-F). These results indicate that MLCK is only partially mediating the intestinal barrier loss pathway after chronic alcohol feeding.

Administration of ethanol lead to an increase of liver weight to body weight ratio in wild type, but not MLCK$^{-/-}$ mice (Suppl. Fig. 13A). Plasma ALT levels as measures for liver injury were reduced in alcohol-fed MLCK$^{-/-}$ mice compared with wild type littermates, but there was no significant difference (Fig. 7A). Hepatic chemokine expression such as Ccl2 (also known as MCP-1) and Ccl3 (MIP-1α) was increased after ethanol treatment in wild type mice but showed comparable level between alcohol fed wild type and MLCK$^{-/-}$ mice (Suppl. Fig. 14). Hepatic fat accumulation was significantly lower in MLCK deficient mice as compared with wild type mice following 8 weeks of ethanol feeding (Fig. 7B-D). However, hepatic triglycerides were still higher in MLCK$^{-/-}$ mice after alcohol as compared with mice fed an isocaloric diet. MLCK deficiency did not affect plasma ethanol levels or hepatic metabolism of ethanol (Fig. 7E and Suppl. Fig. 13B, C). Taken together, MLCK deficiency reduces, but does not completely prevent alcoholic liver disease. These data are consistent with a partial contribution of MLCK to the intestinal barrier loss pathway following chronic alcohol feeding.

Discussion

Although alcoholic liver disease depends on gut derived bacterial products, the mechanism of mucosal barrier disruption and bacterial translocation *in vivo* is unknown. In this study we propose that following chronic alcohol use, monocytes and macrophages in the intestinal lamina propria activate and produce TNFα, both in humans and mouse models. Activation of innate immune cells is dependent on

alcohol-induced dysbiosis. Intestinal barrier disruption and bacterial translocation are facilitated by TNFRI expressed on intestinal epithelial cells. TNFRI-mediated activation of MLCK in enterocytes and disruption of tight junctions partially contributes to reduced barrier function. Increased intestinal permeability results in translocation of microbial products to reach the liver and to promote steatohepatitis (Fig. 7F). This is the first study functionally linking an intestinal gene to gut leakiness and alcoholic liver disease *in vivo*.

Our data indicate that intestinal inflammation initiates the process of intestinal barrier dysfunction and translocation of microbial products during alcoholic liver disease. Intestinal inflammation is also present in the duodenum of patients with liver cirrhosis[28]. But what causes the onset of intestinal inflammation? Inflammasome-mediated enteric dysbiosis results in intestinal inflammation and microbial translocation during the development of NASH. Bacterial products subsequently reach the liver to induce an inflammatory response that promotes progression of NAFLD to NASH[23]. We have previously demonstrated that chronic alcohol feeding is associated with dysbiotic microbiome changes and pronounced intestinal bacterial overgrowth in the jejunum of mice[20]. As shown in our current study, intestinal decontamination not only suppresses intestinal bacterial overgrowth, but it also inhibits intestinal inflammation following alcohol feeding. Currently, we can only speculate about how alcohol-induced dysbiosis triggers intestinal inflammation. Whether bacterial pathogen-associated molecular patterns (PAMP) stimulate innate immune cells in the lamina propria or whether microbial metabolites (e.g. acetaldehyde) affect the innate immune system, requires future studies.

We further demonstrate that TNFRI on enterocytes mediates disruption of the intestinal barrier following chronic alcohol feeding. TNFα is an important immune-mediated tight junction regulator in the intestine[29]. TNFRI, but not TNFR2 deficient mice are protected from chronic liver diseases such as cholestatic liver fibrosis[31] or alcoholic liver disease[26]. Using a bile duct ligation model in mice, we have

previously demonstrated that intestinal TNFRI contributes to protection from cholestatic liver fibrosis by stabilizing the intestinal barrier[16]. However, reactivation of TNFRI specifically on enterocytes increased liver fibrosis as compared with TNFRI mutant mice, but the degree of fibrosis is still lower compared with wild type mice[16] suggesting that liver TNFRI (e.g. on hepatic stellate cells and/or Kupffer cells) might account for differences in the fibrogenic response[30]. In contrast, reactivation of TNFRI on intestinal epithelial cells increased intestinal permeability and liver disease similar to wild type mice after alcohol feeding. These findings support a major role for enteric TNFRI in the disruption of the intestinal barrier during alcoholic liver disease, while hepatic TNFRI expression is dispensable for alcohol-induced liver injury and steatosis. Other hepatic inflammatory mediators such as IL-1β might be more important in inducing downstream effects of TLRs, which are activated by translocated bacterial products. And indeed, IL-1β signaling is required for the development of alcohol-induced liver steatosis, inflammation, and injury as recently reported[31]. TNFR2 is important in regulation disease entities such as experimental inflammatory bowel disease. TNFR2 activates tight junction dysregulation to cause apoptosis-mediated barrier loss in experimental models of colitis[32]. In contrast to colitis models, intestinal inflammation is mild and does not involve an increased intestinal epithelial cell death following chronic alcohol feeding.

MLCK is phosphorylated as a downstream target of TNFα following alcohol administration. MLCK is known to be activated and to play a central role as a common final pathway of barrier disruption in response to TNFα in enterocytes. TNFα-induced MLCK activation triggers caveolin-1-dependent endocytosis and removal of occludin[33]. The role of MLCK in TNFα-induced and disease-associated barrier loss was linked specifically to occludin function[17, 33, 34]. Ethanol stimulated MLCK activation, and the specific MLCK inhibitor ML-7 inhibited both ethanol-induced MLCK activity and tight junction disruption in Caco-2 monolayers[35]. Furthermore, inhibition of MLCK activation with the chemical inhibitor PIK reduced intestinal tight junction disruption and intestinal damage after binge ethanol exposure and burn injury[36]. These studies

suggest that MLCK mediates barrier regulation following an acute ethanol challenge. In contrast, our study using a chronic model of alcohol feeding, intestinal barrier dysfunction, bacterial translocation and alcoholic liver disease are only partially suppressed in MLCK deficient mice. Paracellular permeability is controlled by many tight junction proteins. For example, claudins regulate permeability to specific ions, and the overall ionic permeability is the result of different combination and ratios of claudin proteins[37]. Following chronic alcohol administration tight junction disruption of occludin is prevented in TNFRI mutant and MLCK deficient mice. However, alcohol-induced upregulation of claudin-8 is abrogated in TNFRI mutant mice, while claudin-8 induction is not inhibited in MLCK deficient mice (Suppl. Fig. 15). This indicates that pathways other than MLCK are activated downstream of TNFRI that regulate tight junctions and induce paracellular permeability during chronic stimulation. iNOS could be such a mediator, since it is a known NFκB dependent gene downstream of the TNF-receptor[38]. Indeed, intestinal iNOS expression was lower in TNFRI mutant mice after chronic alcohol feeding, while iNOS protein was similarly in MLCK deficient compared with wild type mice (Suppl. Fig. 16). These data further support that iNOS may serve as another TNF downstream target to mediate alcoholic liver disease.

In conclusion, using tissue specific genetically modified mice, our study is the first to causatively link intestinal permeability to alcoholic liver disease *in vivo*. Alcoholic dysbiosis is associated with intestinal inflammation and is the switch to turn on barrier dysfunction. We identified intestinal TNFRI as master regulator of intestinal barrier function following chronic alcohol administration. Based on this evidence, alcoholic liver disease might be treated by modulating the intestinal microbiome.

Acknowledgements

This study was supported in part by NIH grants K08 DK081830, R01 AA020703, U01 AA021856 and by ABMRF/The Foundation for Alcohol Research (to BS). JRT was supported by R01 DK068271.

References

1. Szabo G, Bala S. Alcoholic liver disease and the gut-liver axis. World J Gastroenterol 2010;16:1321-9.
2. Nanji AA, Khettry U, Sadrzadeh SM, Yamanaka T. Severity of liver injury in experimental alcoholic liver disease. Correlation with plasma endotoxin, prostaglandin E2, leukotriene B4, and thromboxane B2. Am J Pathol 1993;142:367-73.
3. Bjarnason I, Peters TJ, Wise RJ. The leaky gut of alcoholism: possible route of entry for toxic compounds. Lancet 1984;1:179-82.
4. Hritz I, Mandrekar P, Velayudham A, Catalano D, Dolganiuc A, Kodys K, et al. The critical role of toll-like receptor (TLR) 4 in alcoholic liver disease is independent of the common TLR adapter MyD88. Hepatology 2008;48:1224-31.
5. Mathurin P, Deng QG, Keshavarzian A, Choudhary S, Holmes EW, Tsukamoto H. Exacerbation of alcoholic liver injury by enteral endotoxin in rats. Hepatology 2000;32:1008-17.
6. Uesugi T, Froh M, Arteel GE, Bradford BU, Thurman RG. Toll-like receptor 4 is involved in the mechanism of early alcohol-induced liver injury in mice. Hepatology 2001;34:101-8.
7. Rao RK. Acetaldehyde-induced barrier disruption and paracellular permeability in Caco-2 cell monolayer. Methods Mol Biol 2008;447:171-83.
8. Elamin E, Masclee A, Troost F, Dekker J, Jonkers D. Activation of the epithelial-to-mesenchymal transition factor snail mediates acetaldehyde-induced intestinal epithelial barrier disruption. Alcohol Clin Exp Res 2014;38:344-53.
9. Dunagan M, Chaudhry K, Samak G, Rao RK. Acetaldehyde disrupts tight junctions in Caco-2 cell monolayers by a protein phosphatase 2A-dependent mechanism. Am J Physiol Gastrointest Liver Physiol 2012;303:G1356-64.

10. Samak G, Aggarwal S, Rao RK. ERK is involved in EGF-mediated protection of tight junctions, but not adherens junctions, in acetaldehyde-treated Caco-2 cell monolayers. Am J Physiol Gastrointest Liver Physiol 2011;301:G50-9.
11. Suzuki T, Seth A, Rao R. Role of phospholipase Cgamma-induced activation of protein kinase Cepsilon (PKCepsilon) and PKCbetaI in epidermal growth factor-mediated protection of tight junctions from acetaldehyde in Caco-2 cell monolayers. J Biol Chem 2008;283:3574-83.
12. Atkinson KJ, Rao RK. Role of protein tyrosine phosphorylation in acetaldehyde-induced disruption of epithelial tight junctions. Am J Physiol Gastrointest Liver Physiol 2001;280:G1280-8.
13. Banan A, Choudhary S, Zhang Y, Fields JZ, Keshavarzian A. Ethanol-induced barrier dysfunction and its prevention by growth factors in human intestinal monolayers: evidence for oxidative and cytoskeletal mechanisms. J Pharmacol Exp Ther 1999;291:1075-85.
14. Zolotarevsky Y, Hecht G, Koutsouris A, Gonzalez DE, Quan C, Tom J, et al. A membrane-permeant peptide that inhibits MLC kinase restores barrier function in in vitro models of intestinal disease. Gastroenterology 2002;123:163-72.
15. Victoratos P, Lagnel J, Tzima S, Alimzhanov MB, Rajewsky K, Pasparakis M, et al. FDC-specific functions of p55TNFR and IKK2 in the development of FDC networks and of antibody responses. Immunity 2006;24:65-77.
16. Roulis M, Armaka M, Manoloukos M, Apostolaki M, Kollias G. Intestinal epithelial cells as producers but not targets of chronic TNF suffice to cause murine Crohn-like pathology. Proc Natl Acad Sci U S A 2011;108:5396-401.
17. Clayburgh DR, Barrett TA, Tang Y, Meddings JB, Van Eldik LJ, Watterson DM, et al. Epithelial myosin light chain kinase-dependent barrier dysfunction mediates T cell activation-induced diarrhea in vivo. J Clin Invest 2005;115:2702-15.
18. Cao M, Wang P, Sun C, He W, Wang F. Amelioration of IFN-gamma and TNF-alpha-induced intestinal epithelial barrier dysfunction by berberine via

suppression of MLCK-MLC phosphorylation signaling pathway. PLoS One 2013;8:e61944.

19. Madsen KL, Malfair D, Gray D, Doyle JS, Jewell LD, Fedorak RN. Interleukin-10 gene-deficient mice develop a primary intestinal permeability defect in response to enteric microflora. Inflamm Bowel Dis 1999;5:262-70.
20. Yan AW, Fouts DE, Brandl J, Starkel P, Torralba M, Schott E, et al. Enteric dysbiosis associated with a mouse model of alcoholic liver disease. Hepatology 2011;53:96-105.
21. Hartmann P, Chen P, Wang HJ, Wang L, McCole DF, Brandl K, et al. Deficiency of intestinal mucin-2 ameliorates experimental alcoholic liver disease in mice. Hepatology 2013;58:108-19.
22. Bull-Otterson L, Feng W, Kirpich I, Wang Y, Qin X, Liu Y, et al. Metagenomic analyses of alcohol induced pathogenic alterations in the intestinal microbiome and the effect of Lactobacillus rhamnosus GG treatment. PLoS One 2013;8:e53028.
23. Henao-Mejia J, Elinav E, Jin C, Hao L, Mehal WZ, Strowig T, et al. Inflammasome-mediated dysbiosis regulates progression of NAFLD and obesity. Nature 2012;482:179-85.
24. Adachi Y, Moore LE, Bradford BU, Gao W, Thurman RG. Antibiotics prevent liver injury in rats following long-term exposure to ethanol. Gastroenterology 1995;108:218-24.
25. Hartmann P, Haimerl M, Mazagova M, Brenner DA, Schnabl B. Toll-like receptor 2-mediated intestinal injury and enteric tumor necrosis factor receptor I contribute to liver fibrosis in mice. Gastroenterology 2012;143:1330-40 e1.
26. Yin M, Wheeler MD, Kono H, Bradford BU, Gallucci RM, Luster MI, et al. Essential role of tumor necrosis factor alpha in alcohol-induced liver injury in mice. Gastroenterology 1999;117:942-52.
27. Turner JR. Molecular basis of epithelial barrier regulation: from basic mechanisms to clinical application. Am J Pathol 2006;169:1901-9.

28. Du Plessis J, Vanheel H, Janssen CE, Roos L, Slavik T, Stivaktas PI, et al. Activated intestinal macrophages in patients with cirrhosis release NO and IL-6 that may disrupt intestinal barrier function. J Hepatol 2013;58:1125-32.

29. Turner JR. Intestinal mucosal barrier function in health and disease. Nat Rev Immunol 2009;9:799-809.

30. Tarrats N, Moles A, Morales A, Garcia-Ruiz C, Fernandez-Checa JC, Mari M. Critical role of tumor necrosis factor receptor 1, but not 2, in hepatic stellate cell proliferation, extracellular matrix remodeling, and liver fibrogenesis. Hepatology 2011;54:319-27.

31. Petrasek J, Bala S, Csak T, Lippai D, Kodys K, Menashy V, et al. IL-1 receptor antagonist ameliorates inflammasome-dependent alcoholic steatohepatitis in mice. J Clin Invest 2012;122:3476-89.

32. Su L, Nalle SC, Shen L, Turner ES, Singh G, Breskin LA, et al. TNFR2 activates MLCK-dependent tight junction dysregulation to cause apoptosis-mediated barrier loss and experimental colitis. Gastroenterology 2013;145:407-15.

33. Marchiando AM, Shen L, Graham WV, Weber CR, Schwarz BT, Austin JR, 2nd, et al. Caveolin-1-dependent occludin endocytosis is required for TNF-induced tight junction regulation in vivo. J Cell Biol 2010;189:111-26.

34. Su L, Shen L, Clayburgh DR, Nalle SC, Sullivan EA, Meddings JB, et al. Targeted epithelial tight junction dysfunction causes immune activation and contributes to development of experimental colitis. Gastroenterology 2009;136:551-63.

35. Ma TY, Nguyen D, Bui V, Nguyen H, Hoa N. Ethanol modulation of intestinal epithelial tight junction barrier. Am J Physiol 1999;276:G965-74.

36. Zahs A, Bird MD, Ramirez L, Turner JR, Choudhry MA, Kovacs EJ. Inhibition of long myosin light-chain kinase activation alleviates intestinal damage after binge ethanol exposure and burn injury. Am J Physiol Gastrointest Liver Physiol 2012;303:G705-12.

37. Carrozzino F, Pugnale P, Feraille E, Montesano R. Inhibition of basal p38 or JNK activity enhances epithelial barrier function through differential modulation of claudin expression. Am J Physiol Cell Physiol 2009;297:C775-87.

38. Taylor BS, Geller DA. Molecular regulation of the human inducible nitric oxide synthase (iNOS) gene. Shock 2000;13:413-24.

39. Schnabl B, Brenner DA. Interactions Between the Intestinal Microbiome and Liver Diseases. Gastroenterology 2014; 146:1513-24.

Figure Legends

Figure 1. Chronic ethanol administration elevates intestinal TNFα production in mice. C57BL/6 mice were orally fed a control or alcohol diet for 8 weeks. (A) TNFα mRNA level in jejunum (n = 14-19). (B) TNFα mRNA level in isolated lamina propria cells of the jejunum (n = 5-9). (C) Relative amount of $TNF\alpha^+$ inflammatory cells isolated from the jejunum and analyzed by FACS (n = 3-4). *p < 0.05, N.S.: no significance.

Figure 2. Alcohol abuse increases intestinal inflammatory $TNF\alpha^+$ cells in humans. (A) TNFα mRNA expression in duodenal biopsies obtained from healthy controls (n = 15) and patients with chronic alcohol abuse (n = 22). (B and C) Duodenal biopsies obtained from healthy controls (n = 11) and patients with chronic alcohol abuse (n = 8) were stained with CD68 (red) and TNFα (green) by immunofluorescence. Nuclei are stained in blue. (B) Representative intestinal sections are shown (magnification x200). (C) Quantification of CD68/TNFα double positive cells. *p < 0.05.

Figure 3. Intestinal decontamination inhibits alcohol-induced dysbiosis, intestinal inflammation and barrier dysfunction. (A-F) C57BL/6 mice were orally fed a control diet (n = 9), alcohol diet (n = 9) and alcohol diet plus antibiotics (ABX; n = 9). (A) Total cecal bacteria. (B) Jejunal TNFα mRNA level. (C) Quantification of F4/80 TNFα double positive cells in the jejunum as assessed by immunofluorescent staining. (D) Quantification of Lys6C TNFα double positive cells in the jejunum as assessed by immunofluorescent staining. (E) Representative western blot for occludin in the jejunum. (F) Fecal albumin content. (G-H) C57BL/6 mice were orally fed a control or alcohol diet for indicated time points (n = 4-7). (G) Fecal albumin content. Values are presented relative to control-fed animals. (H) Jejunum TNFα mRNA level after 11 days of control and alcohol diet feeding. *p < 0.05, N.S.: no significance.

Figure 4. Reactivation of TNFRI on intestinal epithelial cells mediates

alcohol-induced intestinal permeability in TNFRI mutant mice. Wild type (WT), TNFRI$^{flxneo/flxneo}$ and VillinCre TNFRI$^{flxneo/flxneo}$ mice were orally fed a control (n = 3-4) and alcohol diet (n = 7-9). (A) Fecal albumin content. (B) Western blot for *E. Coli* proteins in liver. (C) Representative western blot for occludin in the jejunum. (D) Occludin quantification of western blots. (E) Representative immunofluorescent staining for occludin; nuclei are stained blue. *p < 0.05.

Figure 5. Reactivation of TNFRI on intestinal epithelial cells promotes alcoholic liver disease in TNFRI mutant mice. Wild type (WT), TNFRI$^{flxneo/flxneo}$ and VillinCre TNFRI$^{flxneo/flxneo}$ mice were orally fed a control (n = 3-4) and alcohol diet (n = 7-9). (A) Representative liver sections after hematoxylin-eosin staining. (B) Plasma ALT level. (C) Representative liver sections after oil red O staining. (D) Hepatic triglyceride content. (E) Plasma ethanol concentration. Magnification x200; *p < 0.05, N.S.: no significance.

Figure 6. MLCK is involved in TNFα signaling and contributes to alcohol-induced barrier loss. (A) Wild type (WT), TNFRI$^{flxneo/flxneo}$ and VillinCre TNFRI$^{flxneo/flxneo}$ male mice were treated with ethanol or dextrose as control (ctlr) by gavage once (n = 3-4). Representative western blot for phosphorylated MLCK (p-MLCK) in epithelial cells isolated from the jejunum. (B-F) MLCK$^{+/+}$ and MLCK$^{-/-}$ littermate mice were orally fed a control (n = 4) and alcohol diet (n = 10-14). (B) Fecal albumin content. (C) Western blot for *E. Coli* proteins in liver (left panel); plasma LPS level (right panel). (D) Representative western blot for occludin in the jejunum. (E) Occludin quantification of western blots. (F) Representative immunofluorescent staining for occludin; nuclei are stained blue. *p < 0.05.

Figure 7. MLCK contributes to alcoholic liver disease. MLCK$^{+/+}$ and MLCK$^{-/-}$ mice were orally fed a control (n = 4) and alcohol diet (n = 10-14). (A) Plasma ALT level. (B) Hepatic triglyceride content. (C) Representative liver sections after hematoxylin-eosin staining. (D) Representative liver sections after oil red O staining. (E) Plasma ethanol

concentration. *p < 0.05. (F) Schematic representation of the proposed model of microbial translocation during alcoholic liver disease: Following the onset of alcoholic dysbiosis, monocytes and macrophages of the intestinal lamina propria are activated and produce TNFα. TNFα binds to TNFRI on enterocytes and increases intestinal permeability. This is in part mediated by the activation of MLCK resulting in disruption of tight junctions. Microbial products cross the mucosal barrier to reach the liver via the portal circulation. Microbial products cause hepatic inflammation and liver disease. The model has been reproduced from[39] with permission from Elsevier and modified with additional permission from Elsevier.

Figure 1

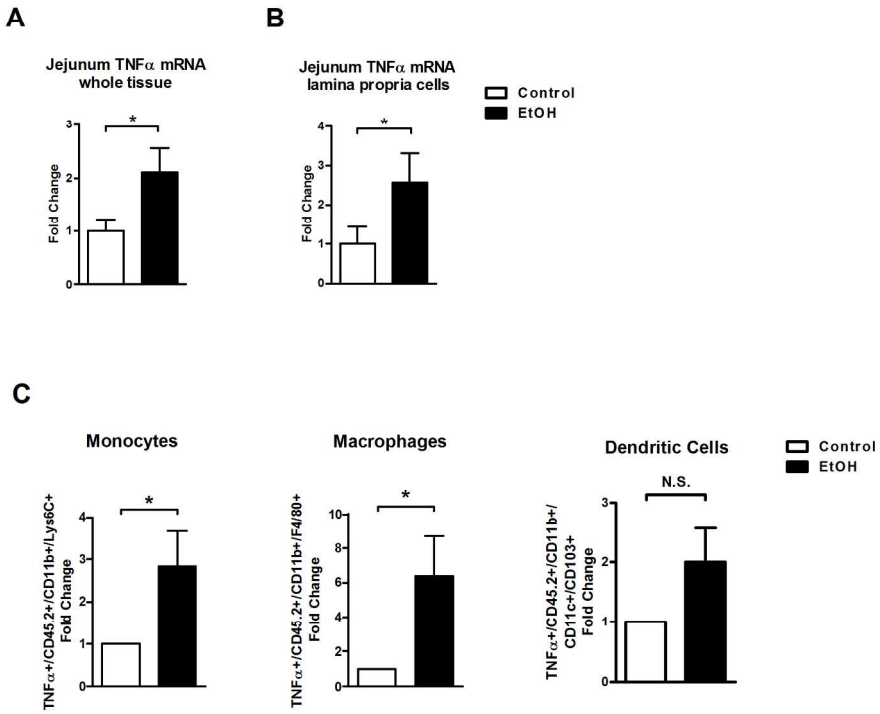

199x199mm (300 x 300 DPI)

Figure 2

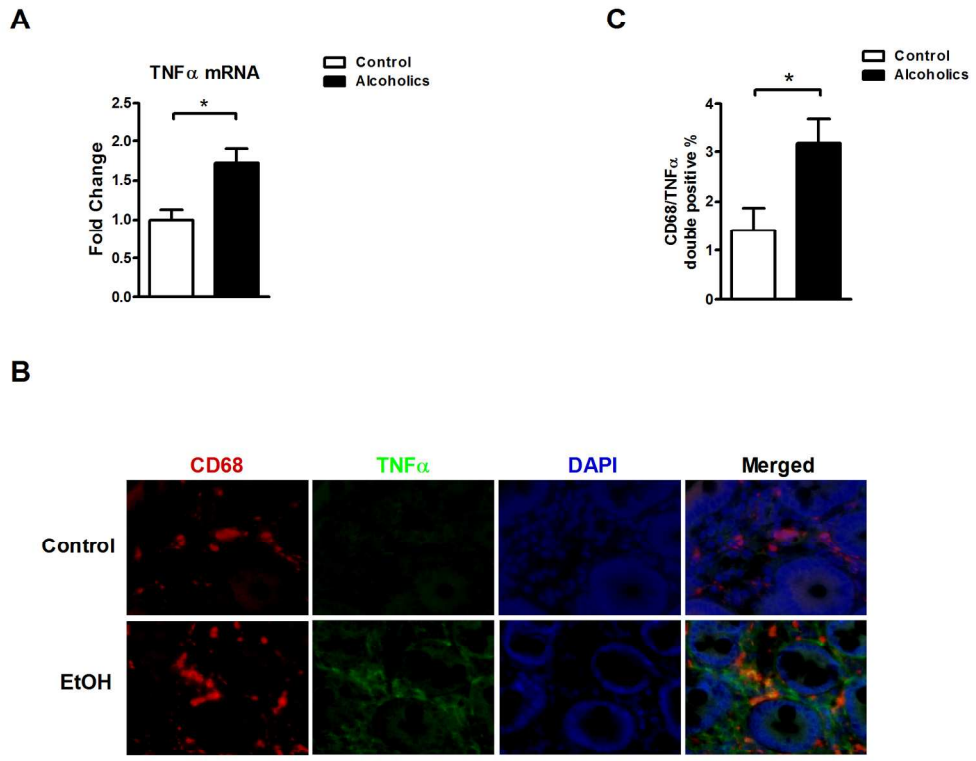

173x162mm (300 x 300 DPI)

Figure 3

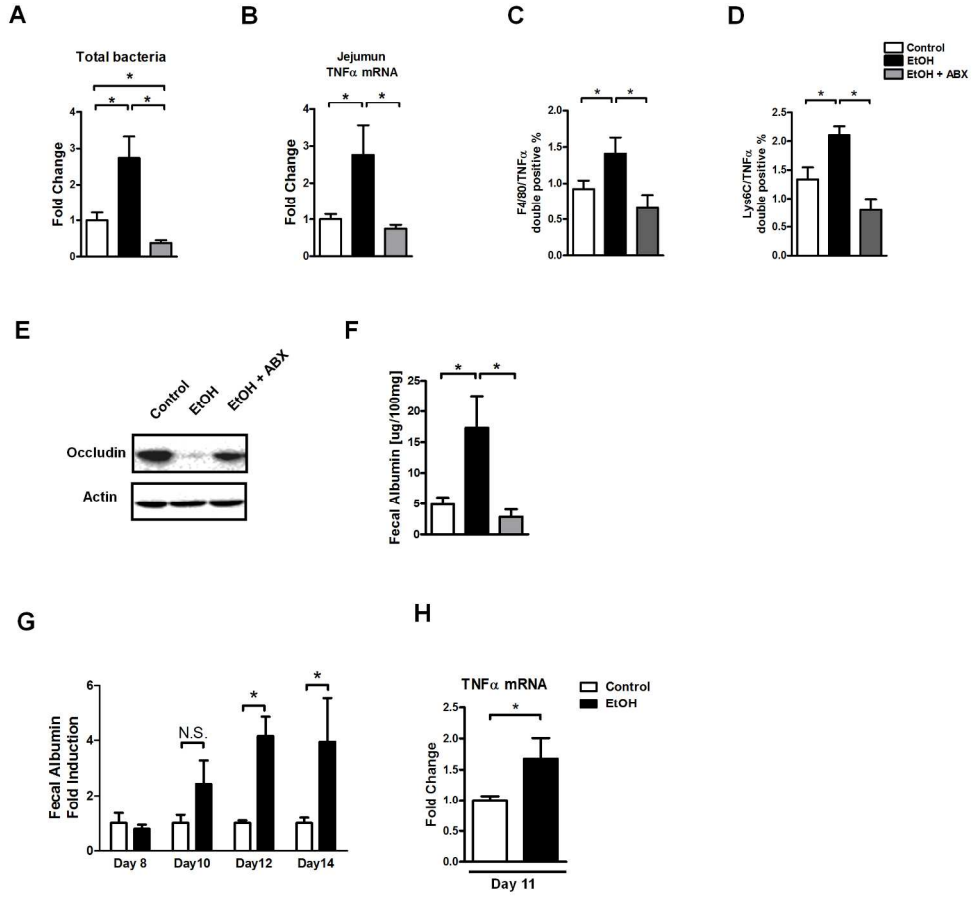

202x202mm (300 x 300 DPI)

Figure 4

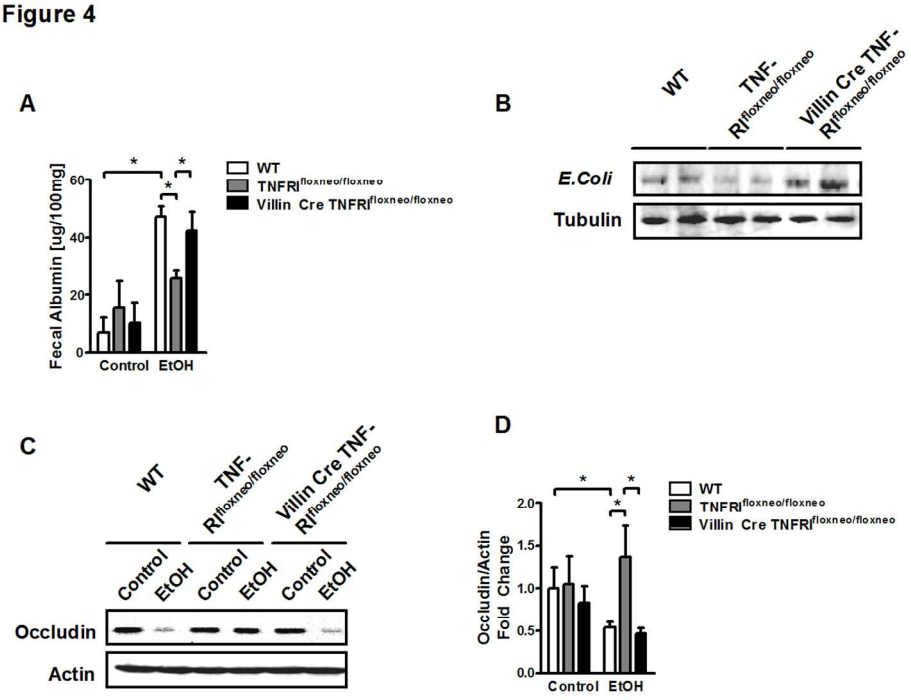

114x147mm (300 x 300 DPI)

Figure 5

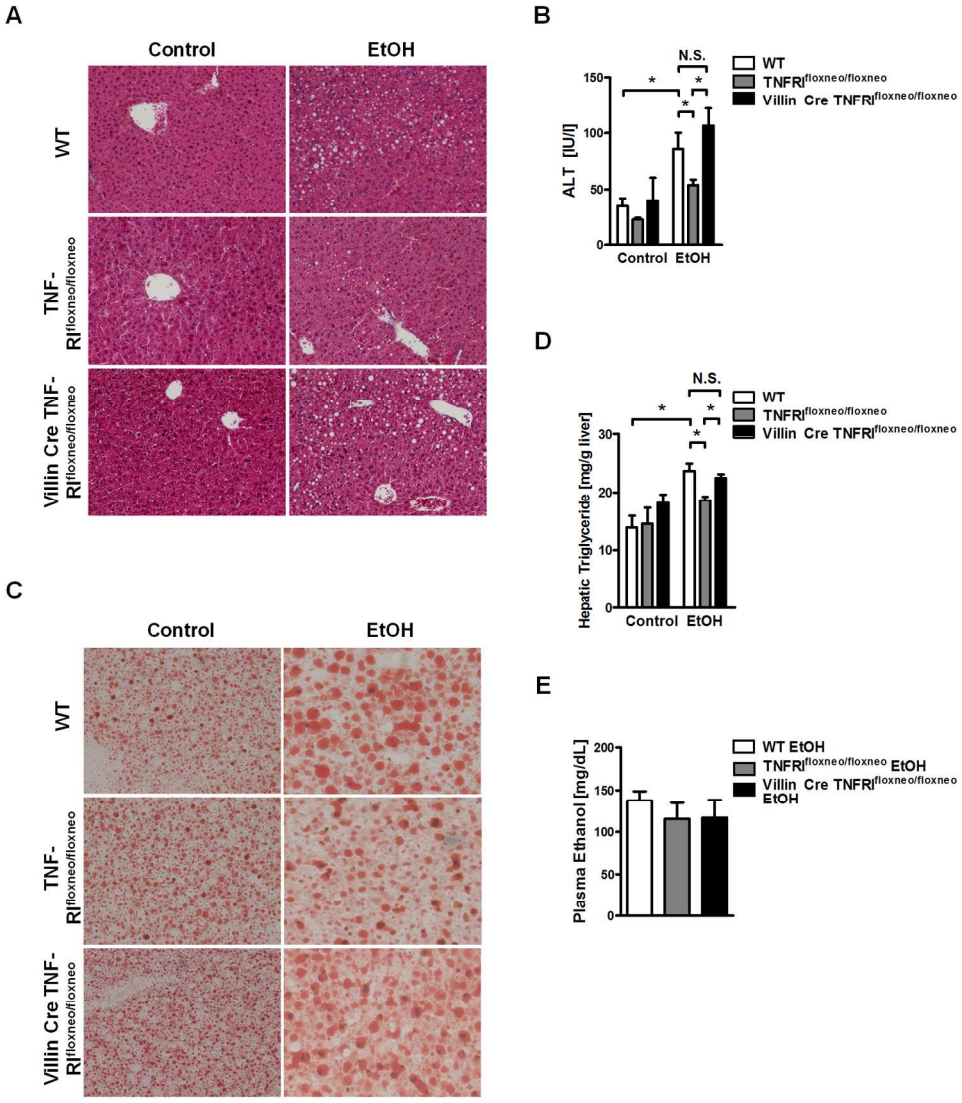

157x189mm (300 x 300 DPI)

Figure 6

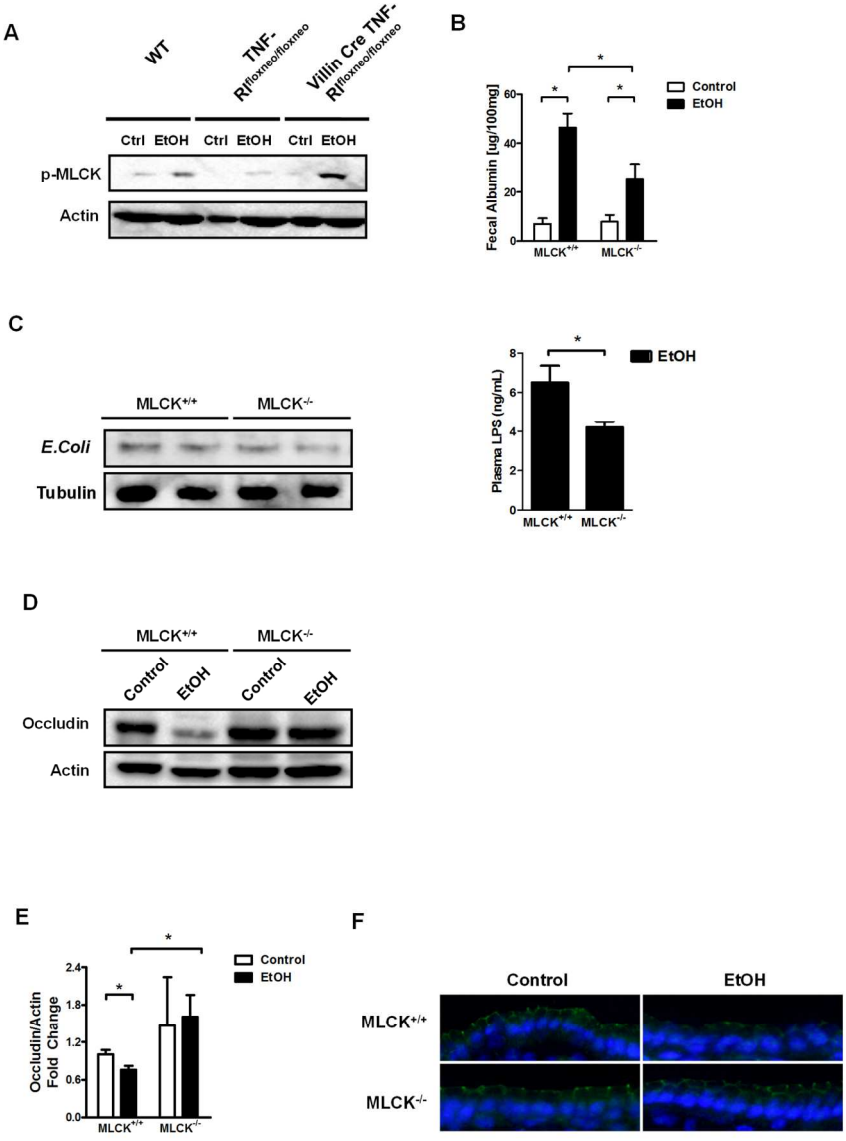

153x208mm (300 x 300 DPI)

Figure 7

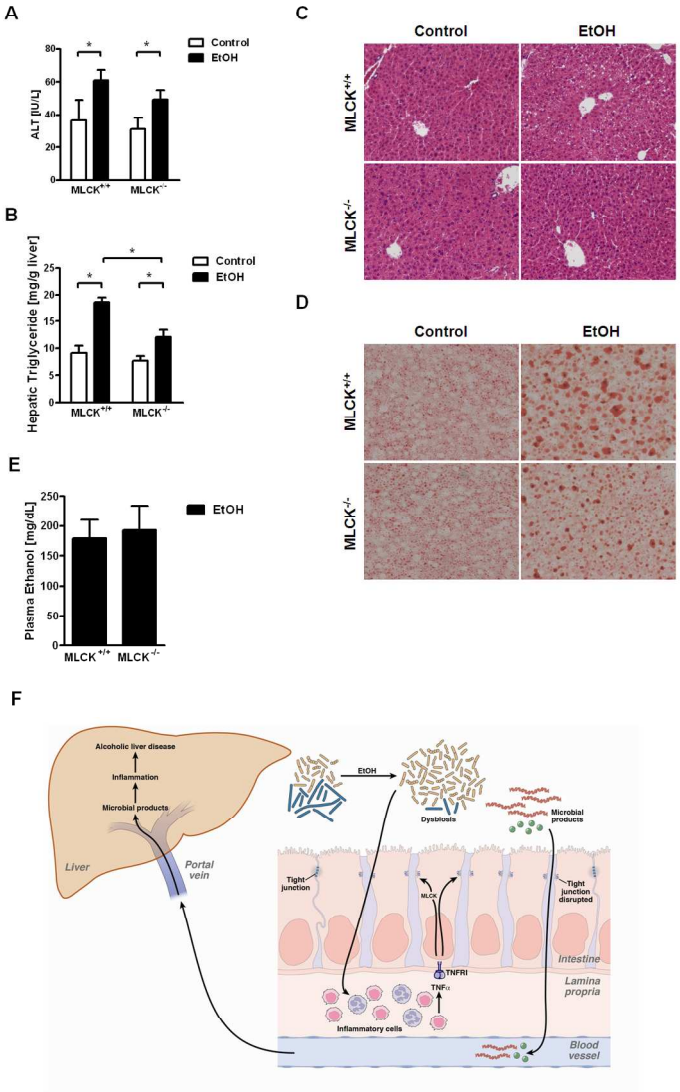

165x198mm (300 x 300 DPI)

Supplementary Materials and Methods

Animal models of alcohol feeding. The Lieber DeCarli diet consisted of administering Micro Stabilized Rod Liq AC IRR (LD101A) and Maltodextrin IRR (9598) from TestDiet and 200 Proof Ethanol from Gold Shield in a specific combination following the manufacturer's feeding directions for two weeks. In brief, the caloric intake from ethanol was 0% on day 1, 10% on day 2 and 3, 20% on day 4 and 5, 30% from day 6 until the end of 6 weeks, and 36% for the last 2 weeks. Mortality of alcohol-fed mice was less than 25% in each ethanol-fed group. Pair-fed control mice received a diet with an isocaloric substitution of dextrose (LD101; TestDiet). Antibiotics treatment was started at 4 weeks after liquid diet feeding, and mice were gavaged daily until harvesting. The composition of antibiotics mixture has been described (Polymyxin B (150 mg/kg BW/day) and Neomycin (200 mg/kg BW/day))[1]. Control mice were gavaged daily with an equal volume of vehicle (water). For acute alcohol treatment, mice were gavaged with 33% ethanol (Vol/Vol) using a dose of 5g/kg, sacrificed at 8 hours after administration, and MLCK phosphorylation was assessed in isolated intestinal epithelial cells. Age-matched female mice were used for the study except when stated otherwise. All animals received humane care in compliance with institutional guidelines.

Human samples. The selection criteria for the patient population with alcohol abuse has been described[2], and biopsies were taken from patients with endoscopically normal duodenums. Written informed consent was obtained from all patients and healthy controls. The study protocol was approved by the Ethics Committee of the Université Catholique de Louvain, in Brussels, Belgium, and of the VA San Diego Healthcare System. Duodenal biopsies were preserved in RNAlater (Qiagen) until RNA extraction using Trizol (Invitrogen). cDNA was synthetized and quantitative PCR was performed with the Step One Plus device (Applied Biosystems) by using SYBR Green PCR Master Mix (Applied Biosystems)[3]. The ΔΔ CT method was used for quantification normalized to ribosomal protein L19 RNA (Rpl19; internal standard). Primers for human TNFα (NM_000594) were designed with Primer Express design

software (Applied Biosystems): 5'-GGAGAAGGGTGACCGACTCA-3'; 5'-TGCCCAGACTCGGCAAAG-3'.

Histological analysis. Formalin fixed tissues were stained with hematoxylin and eosin and analyzed by microscopy. For hepatic lipid accumulation analysis, frozen section was cut and stained with oil red O. TUNEL staining was performed using a commercial kit (Millipore) following manufacturer's instructions.

Biochemical analysis. Plasma alanine aminotransferase (ALT) level was measured by Infinity ALT kit (Thermo Scientific). Plasma ethanol concentration was determined using the Ethanol Assay Kit (BioVision). Liver triglyceride levels were assessed using the triglyceride Liquid Reagents Kit (Pointe Scientific). Hepatic alcohol dehydrogenase (ADH) activity was measured using a commercial kit (BioVision).

Epithelial cell and lamina propria cell isolation. Isolation of intestinal epithelial and lamina propria cells has been described[4]. Lamina propria cells were collected by centrifugation, stained with PerCP-labeled CD11c, Pacific Blue-labeled CD11b, APC-labeled CD45.2, APC-labeled CD103, FITC-labeled Lys6C, PECy7-labeled F4/80, PE-labeled TNFα (all eBiosciences) and further analyzed by FACS analysis.

RNA extraction and realtime PCR analysis. RNA was extracted from mouse tissues using Trizol (Invitrogen). RNA was digested with DNase using the DNA-free kit (Ambion) and reverse transcribed using the High Capacity cDNA Reverse Transcription kit (ABI). Realtime qPCR was performed with Sybr Green (BioRad) supermix using primer sequences obtained from NIH qPrimerDepot. To determine the total bacterial load present in the cecum, the qPCR value of 16S for each sample was multiplied by the total amount of DNA per gram of cecal contents[5].

Protein expression analysis. Liver microsomes were extracted as described[6]. Whole cell lysates were extracted from sterile liver, intestine or intestinal epithelial

cells, and western blot analysis was performed as described using primary antibodies for CYP2E1 (Millipore Corporation), *E. Coli* (DAKO), VDAC1 (Abcam), long isoform of p-MLCK [pS1760] (Invitrogen), iNOS (Santa Cruz), occludin (Invitrogen), TNFRI (Abcam), β-Actin (Sigma-Aldrich), and α-Tubulin (Santa Cruz). All materials used for measuring *E. Coli* proteins in the liver were sterile and pyrogen free. Frozen intestinal sections were stained using the primary antibody anti-occludin and a FITC-conjugated secondary antibody (all Invitrogen). Nuclei are stained with Hoechst (blue). To detect TNFα producing monocytes and macrophages in human duodenal biopsies and animal samples, tissue was stained with primary antibodies against CD68 (DAKO), F4/80 (eBioscience), Lys6C (Abcam) and TNFα (Abcam) and positive reactions were visualized using fluorescent labeled secondary antibodies. 5-6 random high power fields per slide were chosen for analysis, and double positive cells were expressed as percentage of CD68, F4/80 or Lys6C positive cells in the lamina propria. Nuclei are stained with DAPI (blue). Fecal albumin was determined by ELISA (Bethyl Labs) as described[6] . Plasma TNFα was measured using enzyme-linked immunosorbent assay (eBioscience) with a lower detection limit of 15.6 pg/mL.

LPS measurement. Plasma LPS level was measured by a commercial ELISA kit (Cloud-Clone Corp) according to the manufacturer's instruction.

FITC-dextran permeability assay. Mice were fed control or alcohol liquid diet for 2 weeks, and permeability was measured in an isolated jejunal loop as described in detail before[7]. In brief, after anesthesia, a midline laparotomy incision was made. An approximate 4cm long segment of the jejunum was created with two vascular hemoclips without disrupting the mesenteric vascular arcades. The length of intestine between the two clips was injected with 50ml FITC-dextran (4kDa; 100mg/ml; Sigma). After 1 hr, mice were sacrificed and fluorescence was measured in the plasma.

Statistical analysis. Student's *t*-test was used for statistical analysis. All data are presented as mean ± SEM.

Supplementary Figure Legends

Supplementary Figure 1. Chronic ethanol administration does not elevate TNFα production in inflammatory cells in the ileum and colon of mice. C57BL/6 mice were orally fed a control or alcohol diet for 8 weeks (n = 3-4). Relative amount of $TNF\alpha^+$ inflammatory cells isolated from the ileum or colon and analyzed by FACS. N.S.: no significance.

Supplementary Figure 2. Chronic ethanol administration does not elevate numbers of inflammatory cells in the intestine. C57BL/6 mice were orally fed a control or alcohol diet for 8 weeks (n = 3-4). Inflammatory cells isolated from the intestine and analyzed by FACS. *p < 0.05.

Supplementary Figure 3. Intestinal permeability in the jejunum of mice fed alcohol. C57BL/6 mice were orally fed a control or alcohol diet for 2 weeks (n = 20-21 in each group). FITC-dextran (50ml, 100mg/ml) was injected into an isolated jejunal loop. FITC was measured in the plasma 1 hr after injection. *p < 0.05.

Supplementary Figure 4. Intestinal decontamination reduces alcoholic liver disease. C57BL/6 mice were orally fed a control diet (n = 9), alcohol diet (n = 9) and alcohol diet plus antibiotics (ABX; n = 9). (A) Plasma ALT level. (B) Hepatic triglyceride content. (C) Representative liver sections after hematoxylin-eosin and oil red O staining (magnification x100). *p < 0.05.

Supplementary Figure 5. Intestinal decontamination reduces liver/body weight ratio but does not affect ethanol absorption. C57BL/6 mice were orally fed a control diet (n = 9), alcohol diet (n = 9) and alcohol diet plus antibiotics (ABX; n = 9). (A) Liver/body weight ratio. (B) Plasma ethanol concentration. *p < 0.05.

Supplementary Figure 6. Intestinal apoptosis and morphology following chronic alcohol feeding. C57BL/6 mice were orally fed a control or alcohol diet for 8

weeks (n = 3-5). (A) H&E staining and (B) TUNEL staining of jejunal sections. Female rat mammary gland after 3-5 days weaning (provided by the manufacturer) was used as positive control for TUNEL staining.

Supplementary Figure 7. TNFRI expression in liver and intestine. TNFRI protein expression was measured in isolated epithelial cells of the jejunum (A) and in the liver (B) of wild type (WT), TNFRI$^{flxneo/flxneo}$ and VillinCre TNFRI$^{flxneo/flxneo}$ mice.

Supplementary Figure 8. TNFRI gene expression in enterocytes is not affected by ethanol feeding. C57BL/6 mice were orally fed a control diet (n = 5) and alcohol diet (n = 4-5). Intestinal epithelial cells were isolated from jejunum, ileum and colon, and qPCR for TNFRI performed.

Supplementary Figure 9. TNFa expression is independent from intestinal TNFRI. Wild type (WT), TNFRI$^{flxneo/flxneo}$ and VillinCre TNFRI$^{flxneo/flxneo}$ mice were orally fed alcohol diet (n = 5) for 8 weeks. (A) TNFa mRNA level in the jejunum. (B) Quantification of F4/80 TNFα double positive cells in the jejunum as assessed by immunofluorescent staining. (C) Quantification of Lys6C TNFα double positive cells in the jejunum as assessed by immunofluorescent staining. N.S.: no significance.

Supplementary Figure 10. Plasma TNFα is below the detection level in control and alcohol fed mice. C57BL/6 mice were orally fed a control diet (n = 8) and alcohol diet (n = 9). Plasma TNFα levels were below the detection limit of 15.6 pg/ml.

Supplementary Figure 11. Reactivation of TNFRI on intestinal epithelial cells increases liver/body weight ratio but does not affect ethanol metabolism in TNFRI mutant mice after chronic alcohol feeding. Wild type (WT), TNFRI$^{flxneo/flxneo}$ and VillinCre TNFRI$^{flxneo/flxneo}$ mice were orally fed a control (ctrl; n = 3-4) and alcohol diet (n = 7-9). (A) Liver/body weight ratio. (B) Hepatic alcohol dehydrogenase (ADH) activity. (C) Representative western blot for hepatic microsomal CYP2E1. *$p < 0.05$.

Supplementary Figure 12. TNFR2 is dispensable for intestinal MLCK activation after alcohol administration. Wild type and TNFR2 deficient mice were gavaged with ethanol or dextrose as control once. Western blot for phosphorylated MLCK was performed (p-MLCK) in epithelial cells isolated from the jejunum.

Supplementary Figure 13. Liver/body weight ratio and hepatic ethanol metabolism in MLCK$^{+/+}$ and MLCK$^{-/-}$ mice. MLCK$^{+/+}$ and MLCK$^{-/-}$ littermate mice were orally fed a control (ctrl; n = 4) and alcohol diet (n = 10-14). (A) Liver/body weight ratio. (B) Hepatic alcohol dehydrogenase (ADH) activity. (C) Representative western blot for hepatic microsomal CYP2E1. *$p < 0.05$.

Supplementary Figure 14. MLCK does not affect hepatic chemokine expression after alcohol feeding. MLCK$^{+/+}$ and MLCK$^{-/-}$ littermate mice were orally fed a control (ctrl; n = 4) and alcohol diet (n = 8-10). Hepatic Ccl2 mRNA (A) and Ccl3 mRNA (B) levels. *$p < 0.05$.

Supplementary Figure 15. Claudin-8 expression is differently regulated in TNFRI mutant and MLCK knockout mice following alcohol feeding. (A) Wild type (WT), TNFRI$^{flxneo/flxneo}$ and VillinCre TNFRI$^{flxneo/flxneo}$ mice, (B) MLCK$^{+/+}$ and MLCK$^{-/-}$ mice were orally fed a control (n = 3-4) and alcohol diet (n = 7-10). Claudin-8 mRNA level was measured in the jejunum. *$p < 0.05$, N.S.: no significance.

Supplementary Figure 16. iNOS expression is regulated by TNFRI but not MLCK after chronic alcohol feeding. Wild type (WT), TNFRI$^{flxneo/flxneo}$ and VillinCre TNFRI$^{flxneo/flxneo}$ mice; MLCK$^{+/+}$ and MLCK$^{-/-}$ mice were orally fed a control and alcohol diet for 8 weeks. iNOS protein levels were detected in the jejunum using western blotting.

References

1. Adachi Y, Moore LE, Bradford BU, Gao W, Thurman RG. Antibiotics prevent liver injury in rats following long-term exposure to ethanol. Gastroenterology 1995;108:218-24.

2. Badaoui A, De Saeger C, Duchemin J, Gihousse D, de Timary P, Starkel P. Alcohol dependence is associated with reduced plasma and fundic ghrelin levels. Eur J Clin Invest 2008;38:397-403.

3. Starkel P, Bishop K, Horsmans Y, Strain AJ. Expression and DNA-binding activity of signal transducer and activator of transcription 3 in alcoholic cirrhosis compared to normal liver and primary biliary cirrhosis in humans. Am J Pathol 2003;162:587-96.

4. Hartmann P, Haimerl M, Mazagova M, Brenner DA, Schnabl B. Toll-like receptor 2-mediated intestinal injury and enteric tumor necrosis factor receptor I contribute to liver fibrosis in mice. Gastroenterology 2012;143:1330-40 e1.

5. Yan AW, Fouts DE, Brandl J, Starkel P, Torralba M, Schott E, et al. Enteric dysbiosis associated with a mouse model of alcoholic liver disease. Hepatology 2011;53:96-105.

6. Hartmann P, Chen P, Wang HJ, Wang L, McCole DF, Brandl K, et al. Deficiency of intestinal mucin-2 ameliorates experimental alcoholic liver disease in mice. Hepatology 2013;58:108-19.

7. Fouts DE, Torralba M, Nelson KE, Brenner DA, Schnabl B. Bacterial translocation and changes in the intestinal microbiome in mouse models of liver disease. J Hepatol 2012;56:1283-92.

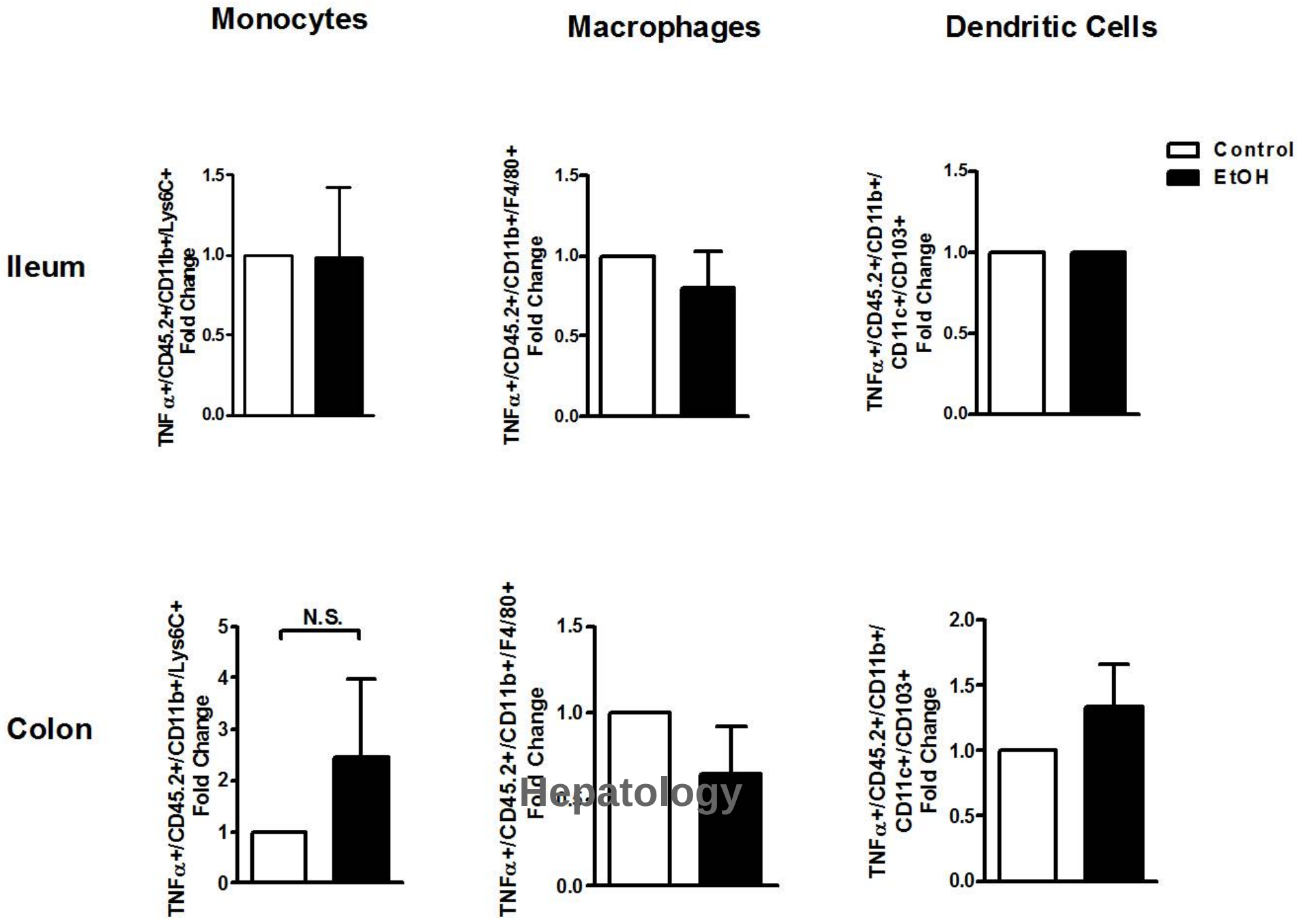
Monocytes
Macrophages
Dendritic Cells
Control
EtOH
Ileum
Colon
TNFα+/CD45.2+/CD11b+/Lys6C+ Fold Change
TNFα+/CD45.2+/CD11b+/F4/80+ Fold Change
TNFα+/CD45.2+/CD11b+/CD11c+/CD103+ Fold Change
N.S.
1.5
1.0
0.5
0.0
5
4
3
2
1
0
2.0

Supplementary Figure 2

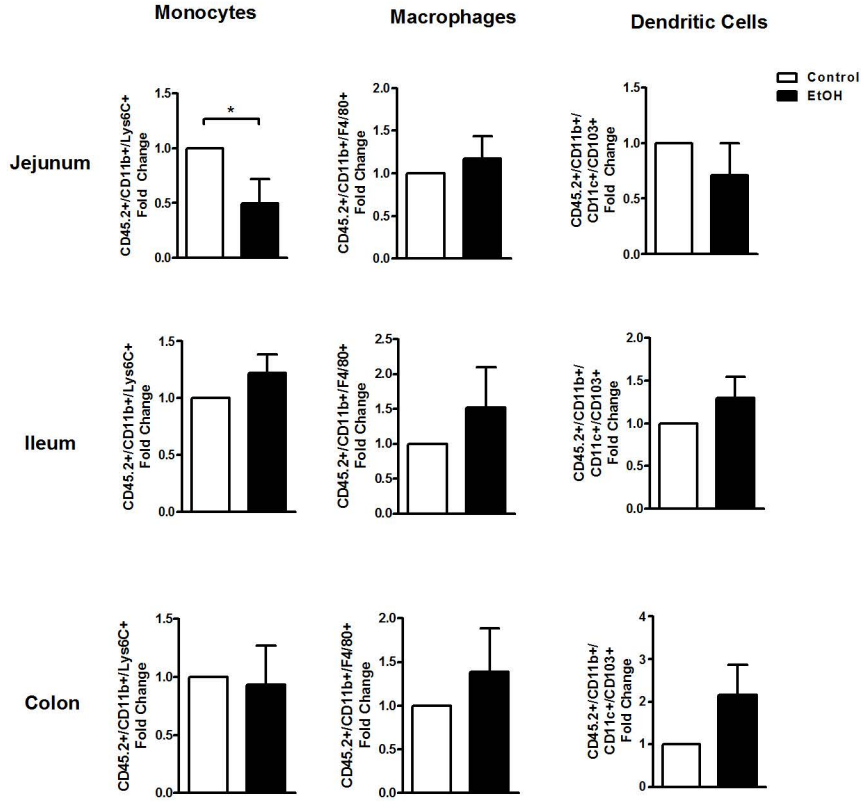

Supplementary Figure 3

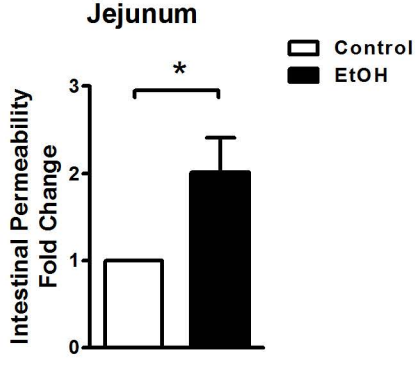

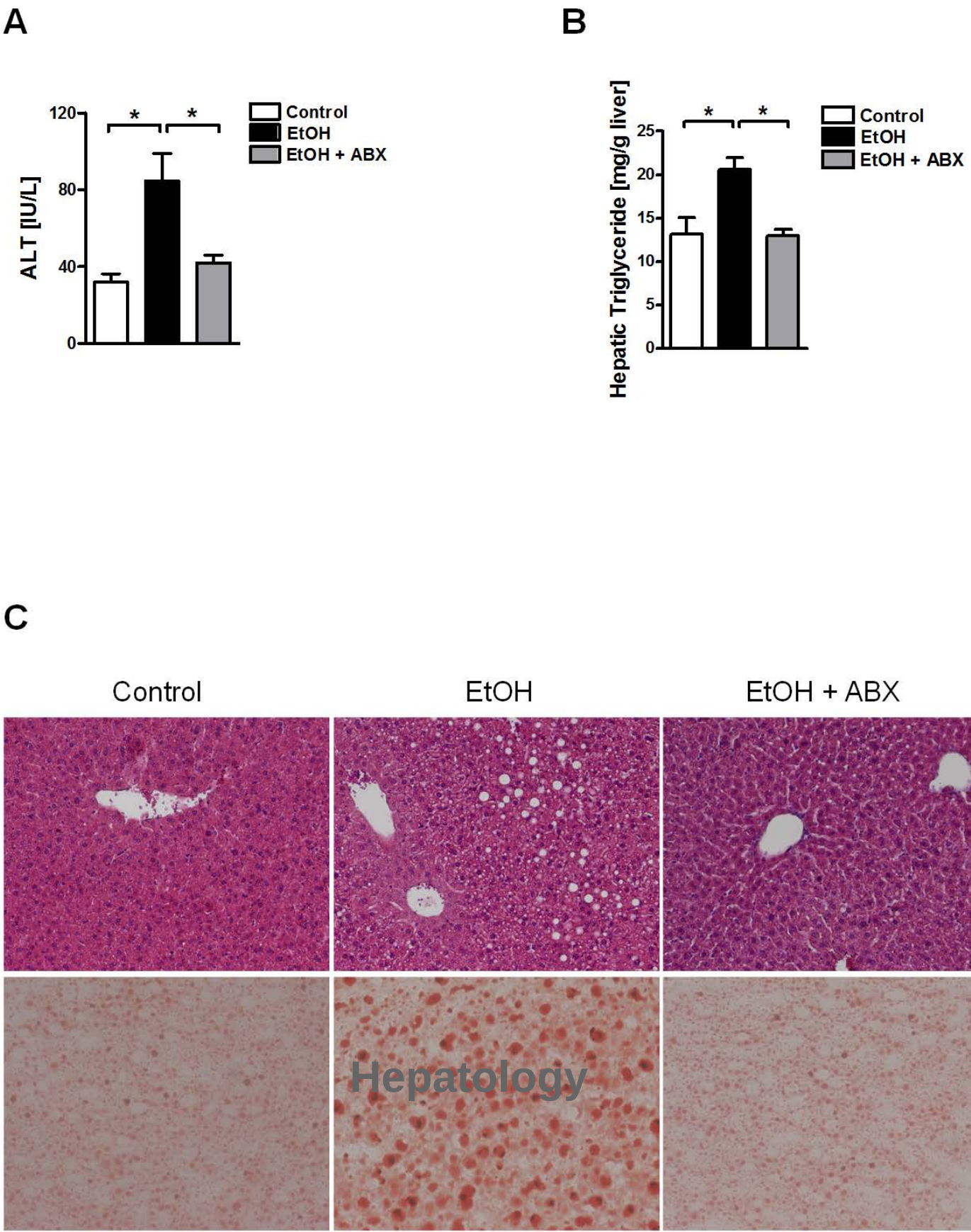
A
ALT [IU/L]
120
80
40
0
*
*
Control
EtOH
EtOH + ABX
B
Hepatic Triglyceride [mg/g liver]
25
20
15
10
5
0
*
*
Control
EtOH
EtOH + ABX
C
Control
EtOH
EtOH + ABX
H & E
Oil Red O
Hepatology

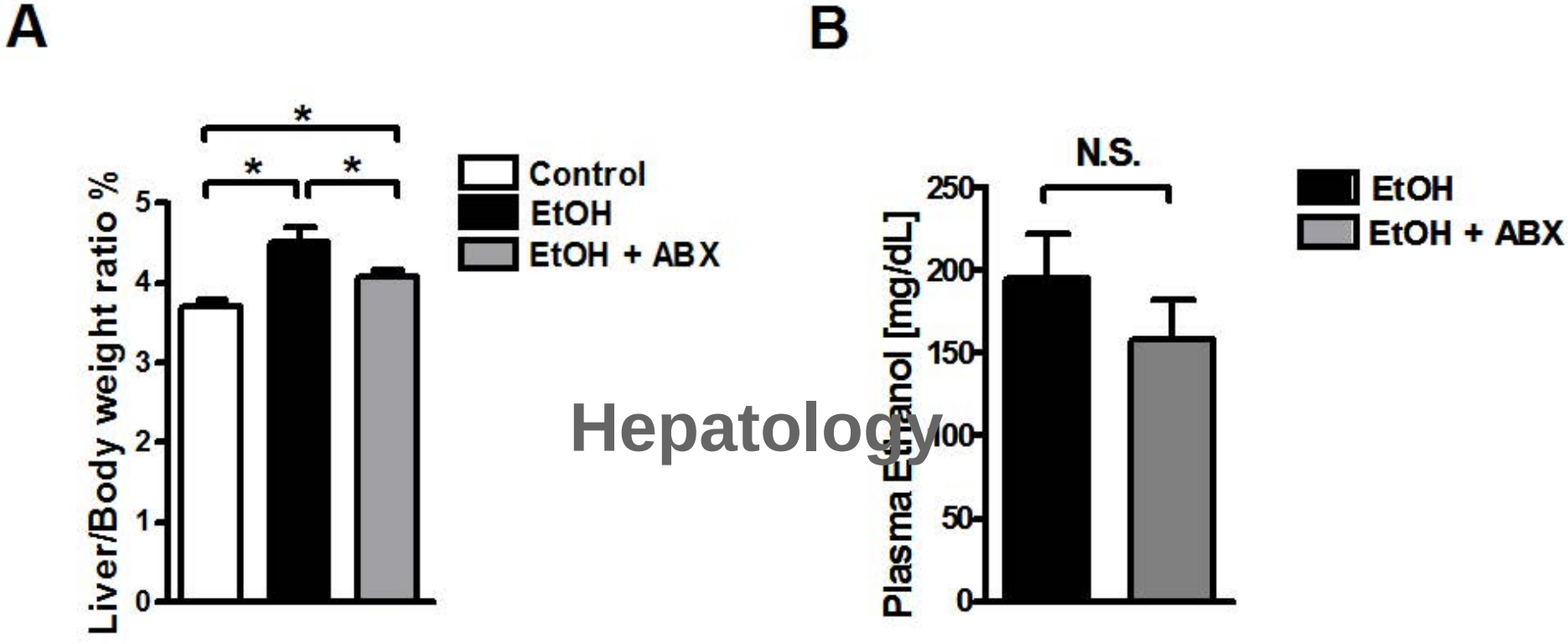
A
B
*
*
*
Control
EtOH
EtOH + ABX
Liver/Body weight ratio %
0
1
2
3
4
5
N.S.
EtOH
EtOH + ABX
Plasma Ethanol [mg/dL]
0
50
100
150
200
250

Supplementary Figure 6

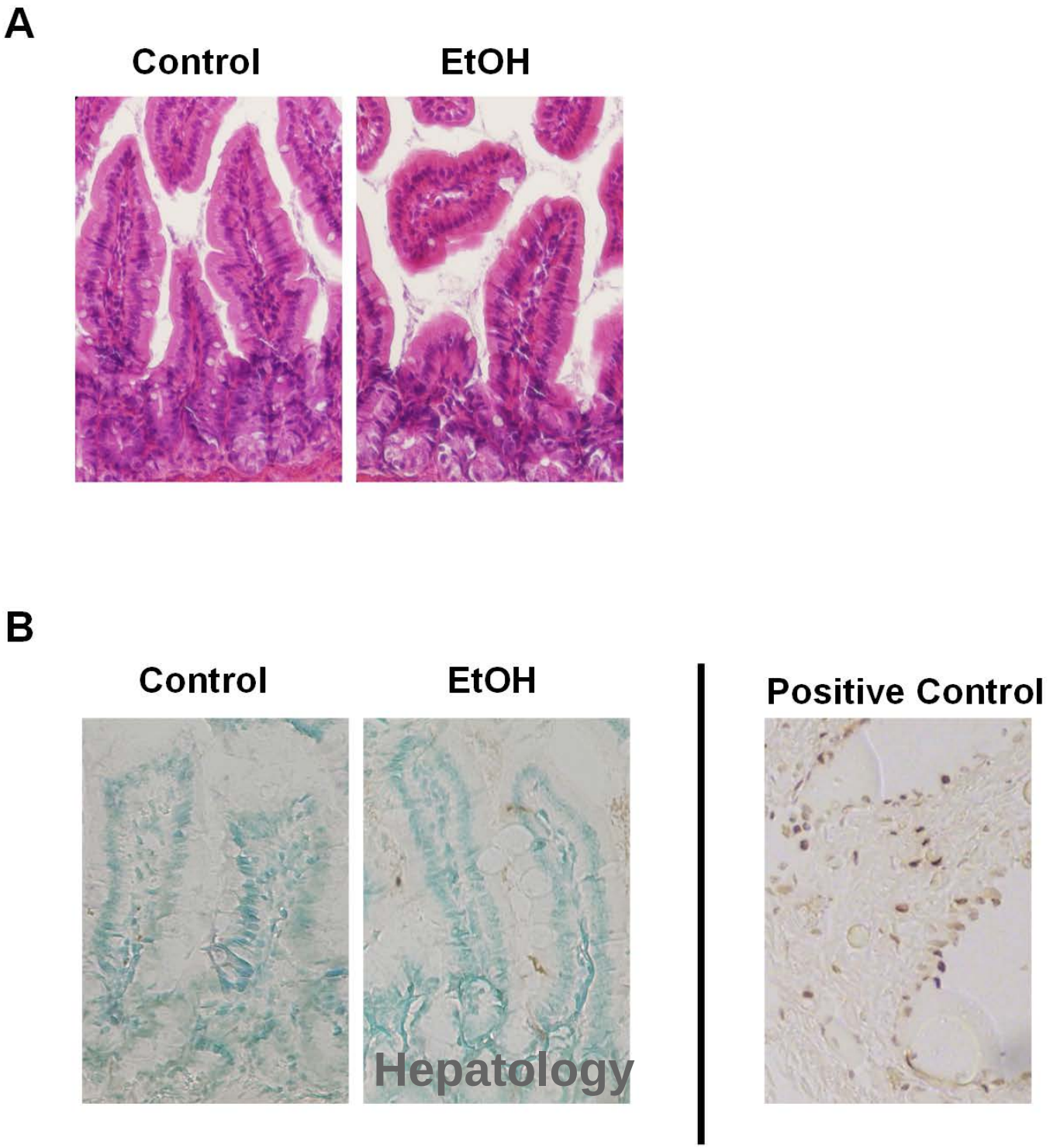

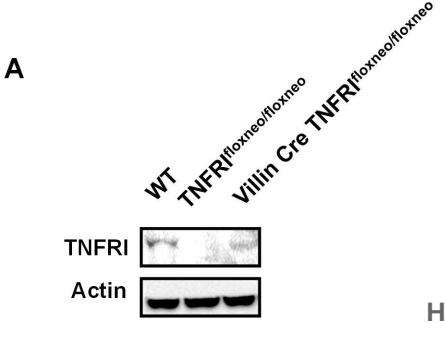
A
WT
TNFRI floxneo/floxneo
Villin Cre TNFRI floxneo/floxneo
TNFRI
Actin

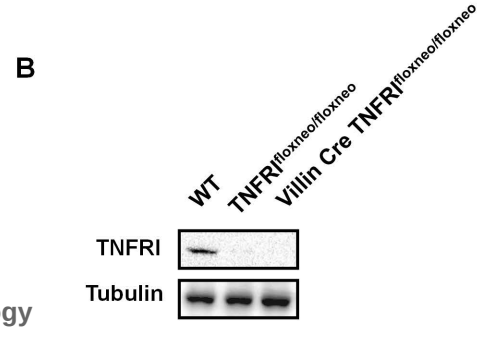
B
WT
TNFRI floxneo/floxneo
Villin Cre TNFRI floxneo/floxneo
TNFRI
Tubulin

Supplementary Figure 8

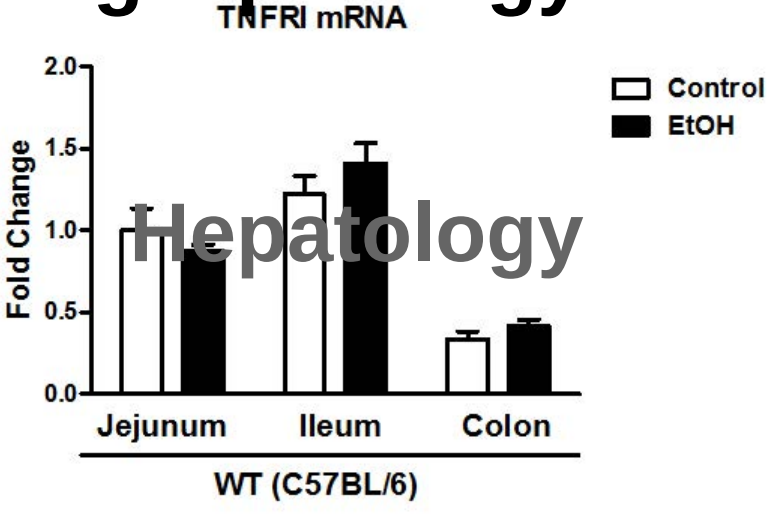

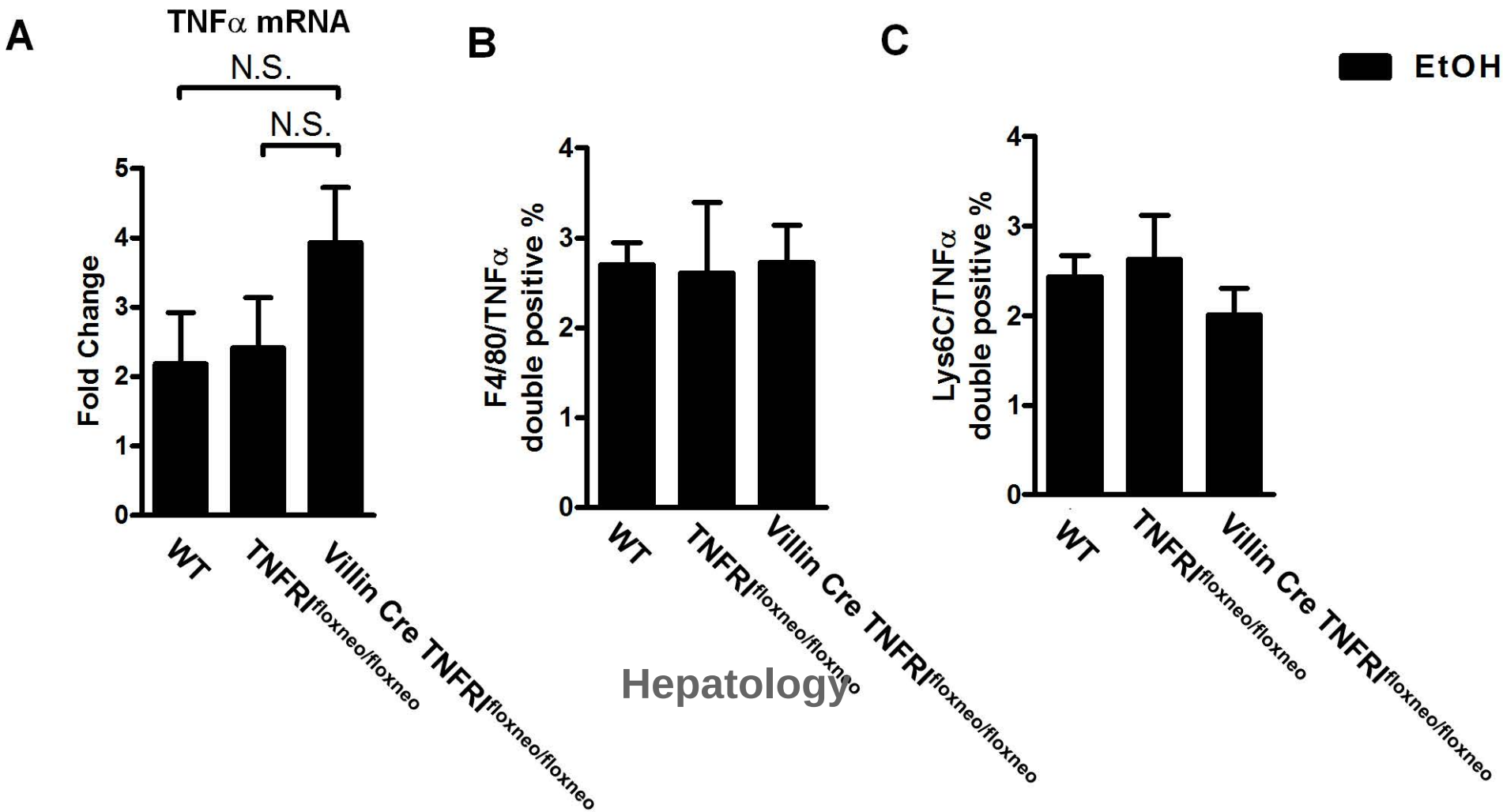
A
TNFα mRNA
N.S.
N.S.
Fold Change
0
1
2
3
4
5
WT
TNFRI floxneo/floxneo
Villin Cre TNFRI floxneo/floxneo
B
F4/80/TNFα double positive %
0
1
2
3
4
WT
TNFRI floxneo/floxneo
Villin Cre TNFRI floxneo/floxneo
C
EtOH
Lys6C/TNFα double positive %
0
1
2
3
4
WT
TNFRI floxneo/floxneo
Villin Cre TNFRI floxneo/floxneo

Supplementary Figure 10

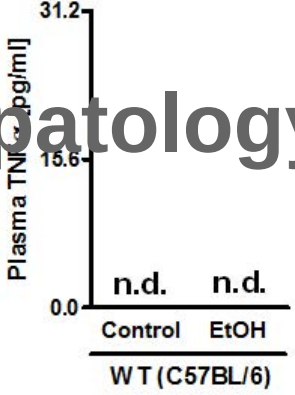

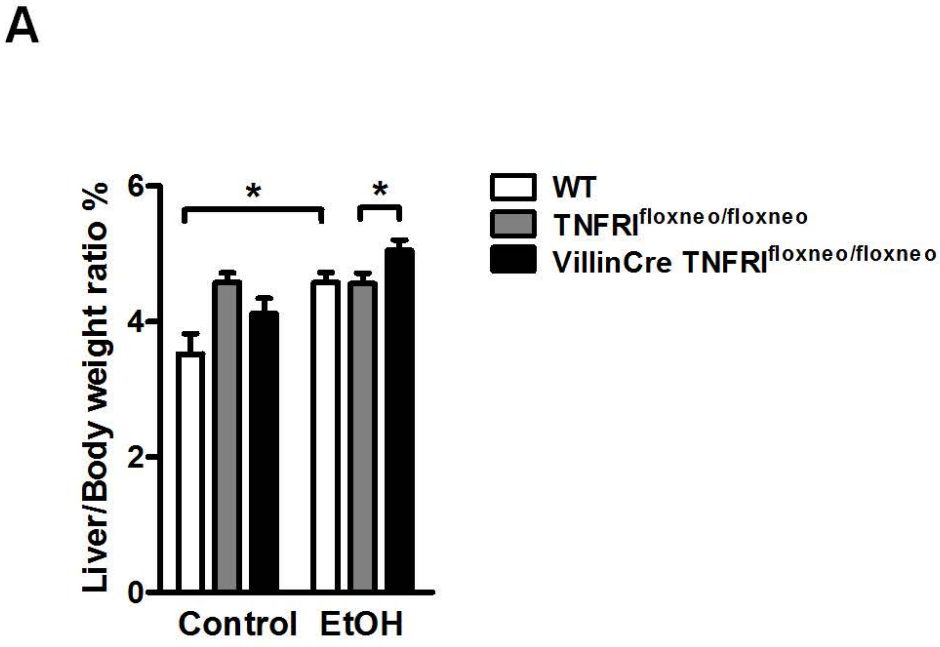
A
Liver/Body weight ratio %
6
4
2
0
*
*
Control
EtOH
WT
TNFRI floxneo/floxneo
VillinCre TNFRI floxneo/floxneo

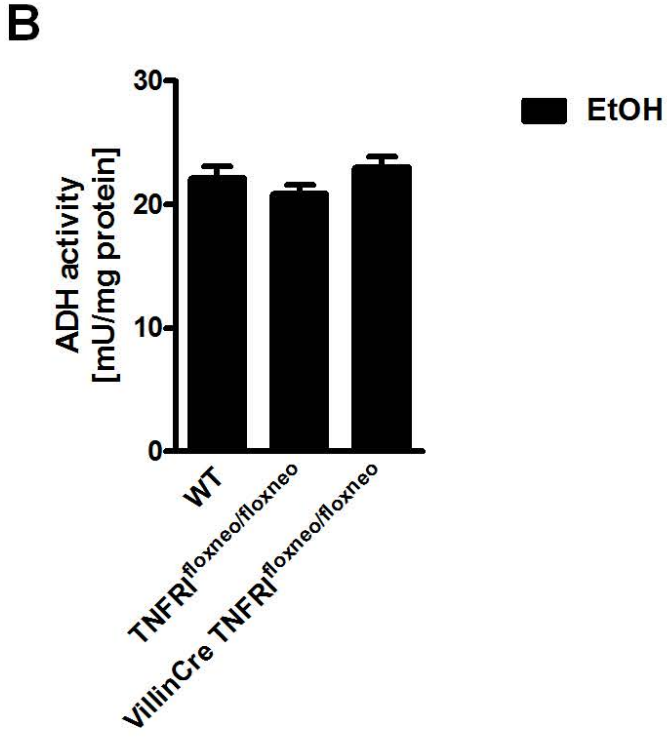
B
ADH activity [mU/mg protein]
30
20
10
0
EtOH
WT
TNFRI floxneo/floxneo
VillinCre TNFRI floxneo/floxneo

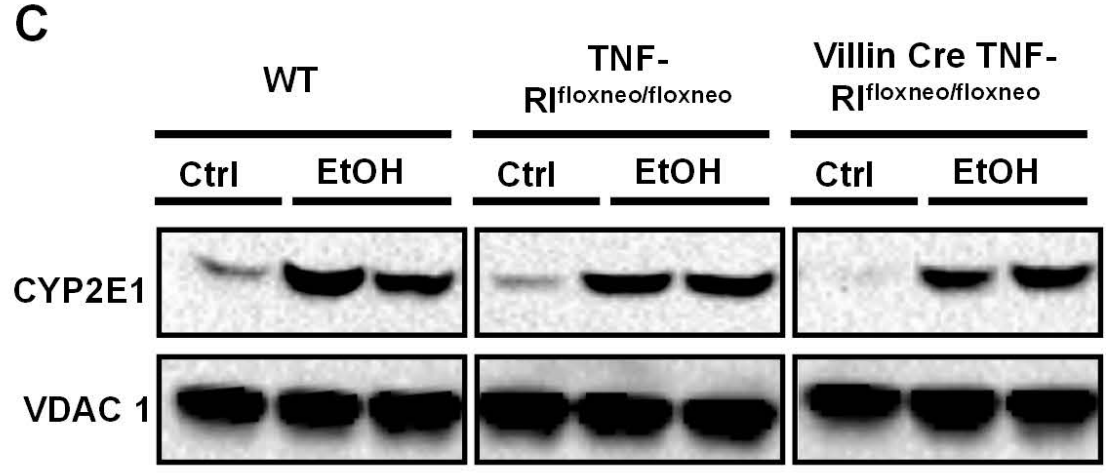
C
WT
TNF-RI floxneo/floxneo
Villin Cre TNF-RI floxneo/floxneo
Ctrl
EtOH
Ctrl
EtOH
Ctrl
EtOH
CYP2E1
VDAC 1

Supplementary Figure 12.

A

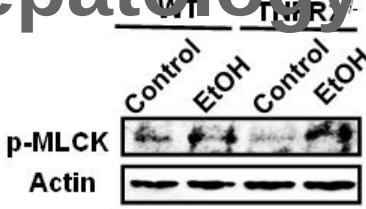

Supplementary Figure 13

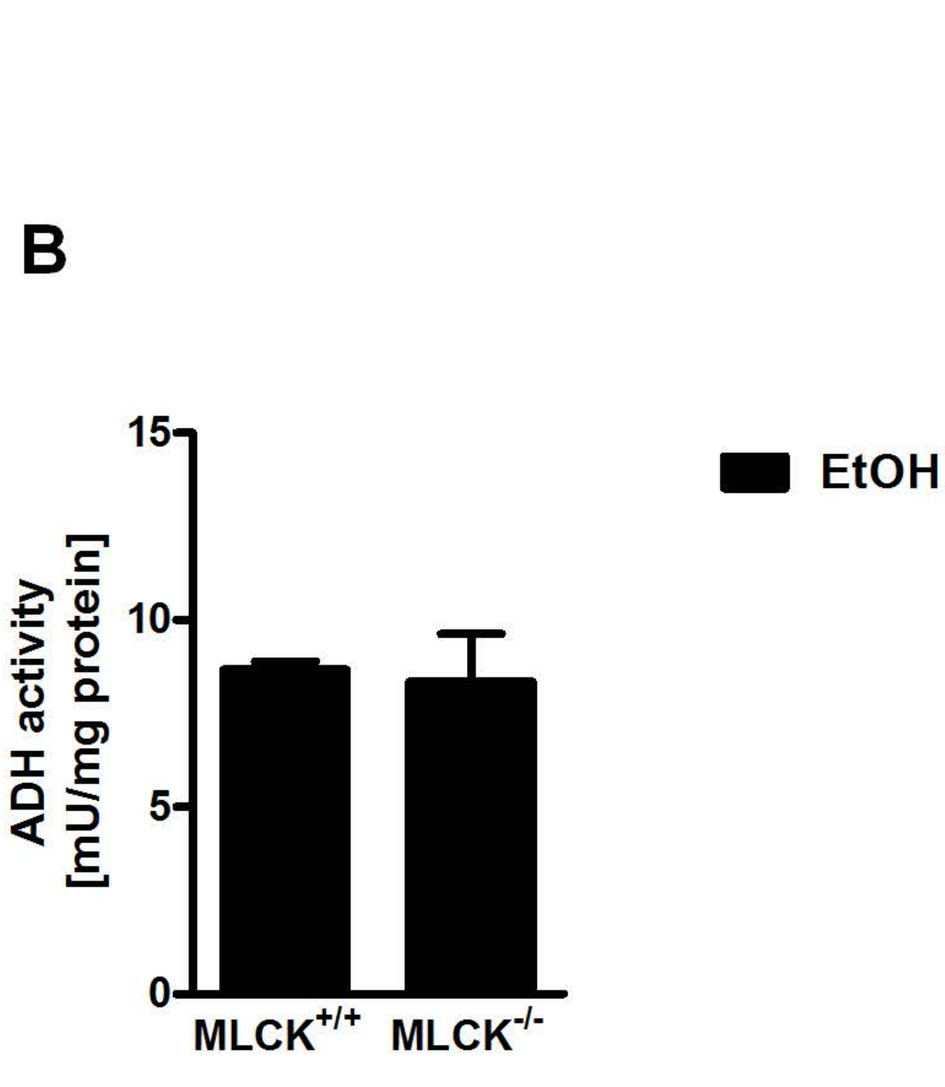

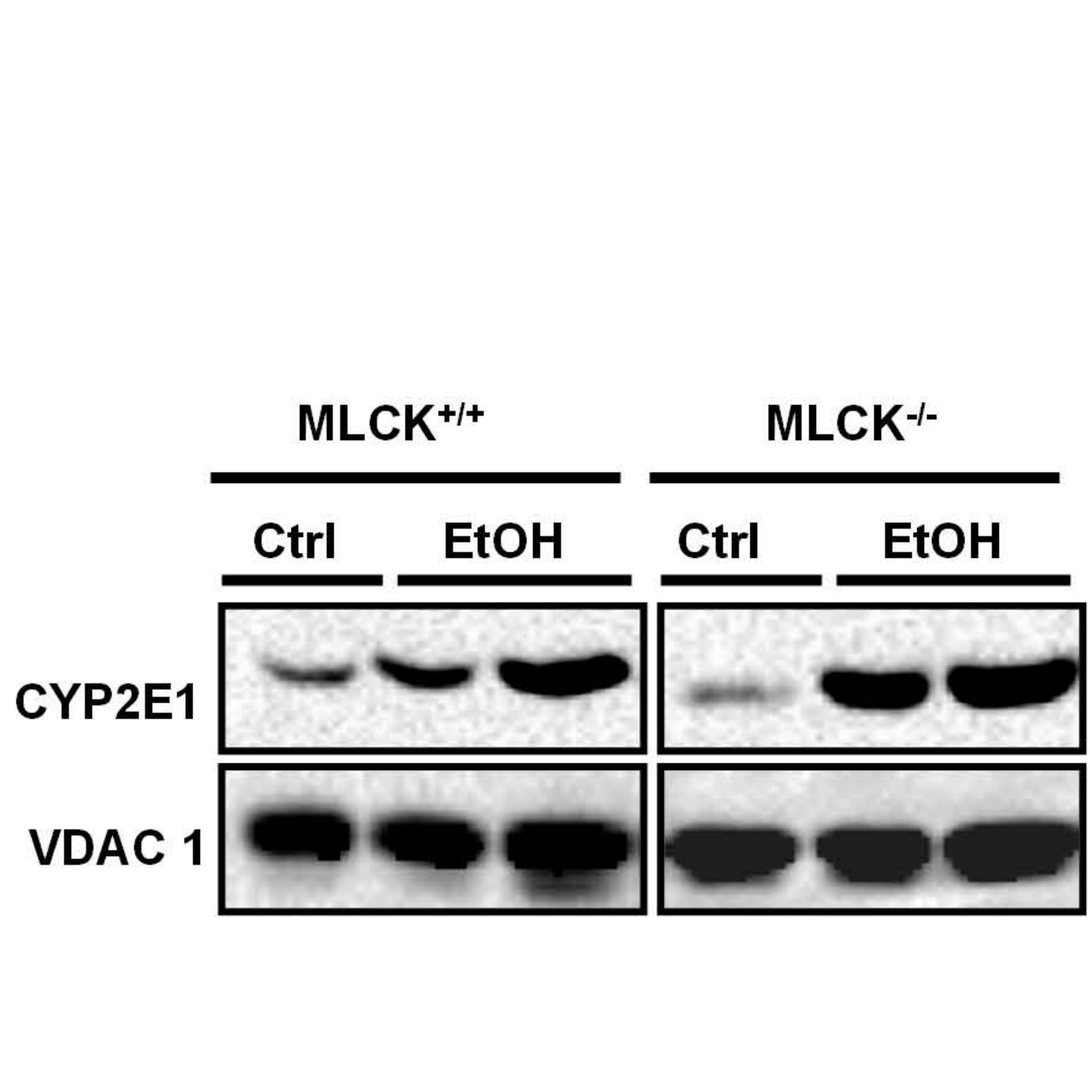

Supplementary Figure 14

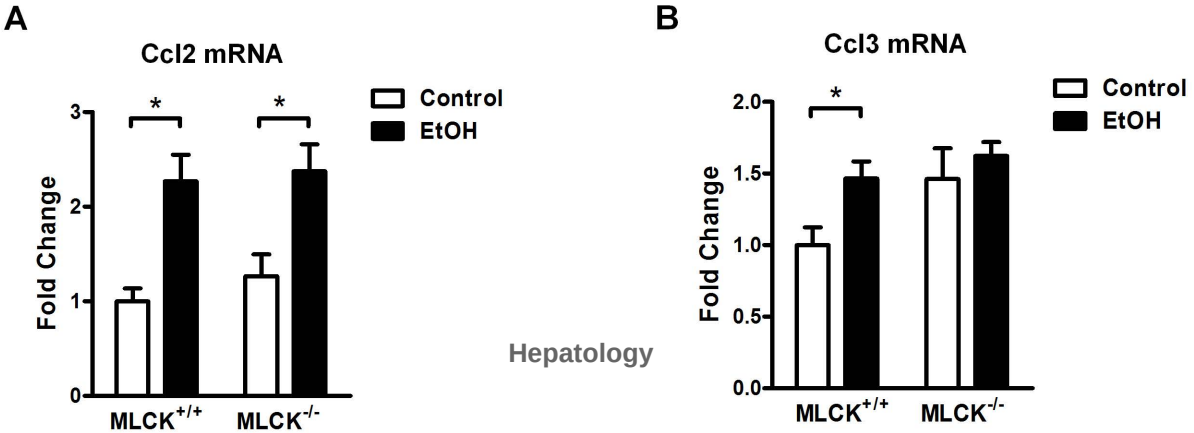

Hepatology

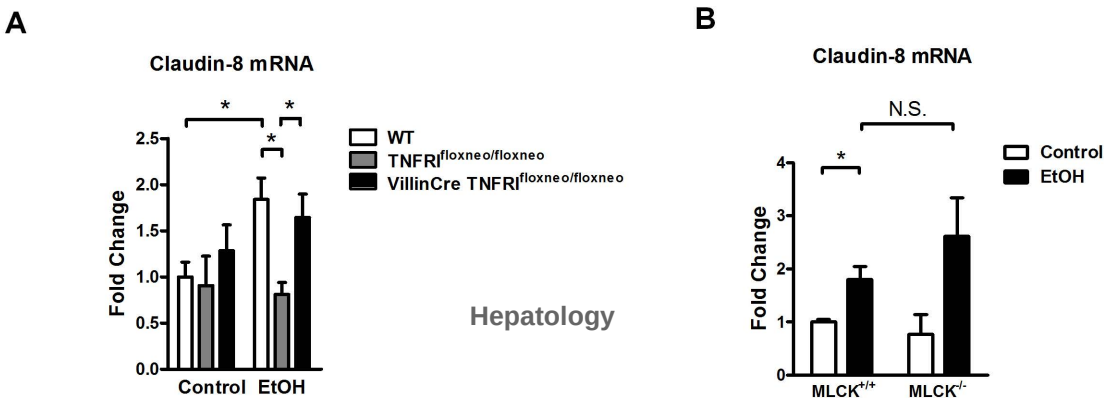
A
Claudin-8 mRNA
Fold Change
2.5
2.0
1.5
1.0
0.5
0.0
Control
EtOH
*
*
*
WT
TNFRI floxneo/floxneo
VillinCre TNFRI floxneo/floxneo
Hepatology
B
Claudin-8 mRNA
N.S.
*
Control
EtOH
Fold Change
4
3
2
1
0
MLCK+/+
MLCK-/-

Supplementary Figure 16

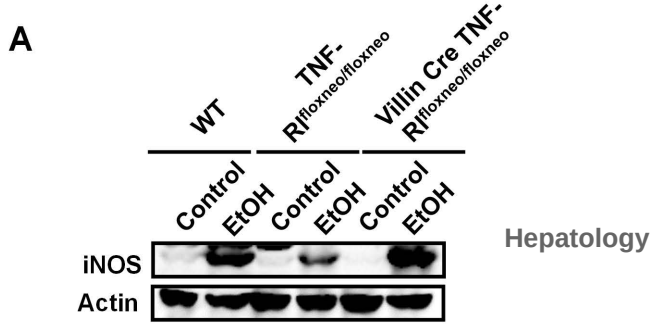

Hepatology